Supplementary Information

A theoretical study on methanol to propene mechanism catalyzed by phosphorus modified acidic FAU zeolite

Mengya Xia[†], Qiaoxian Tong[†], Huai Sun[††], Yingxin Sun[†], Sheng Han*[†], Qianggen Li*[†††]*

[†]School of Chemical and Environmental Engineering, Shanghai Institute of Technology, Shanghai 201418, China

[††]School of Chemistry and Chemical Engineering, Shanghai Jiao Tong University, Shanghai 201418, China

[†††]College of Chemistry and Material Science, Sichuan Normal University, Chengdu 610068, China

*Corresponding authors: Yingxin Sun, Sheng Han, Qianggen Li

Tel: +86-21-6087-7214, +86-28-8476-0802

E-mail: sunyingxin0312@sit.edu.cn, hansheng654321@sina.com, liqgen@sicnu.edu.cn

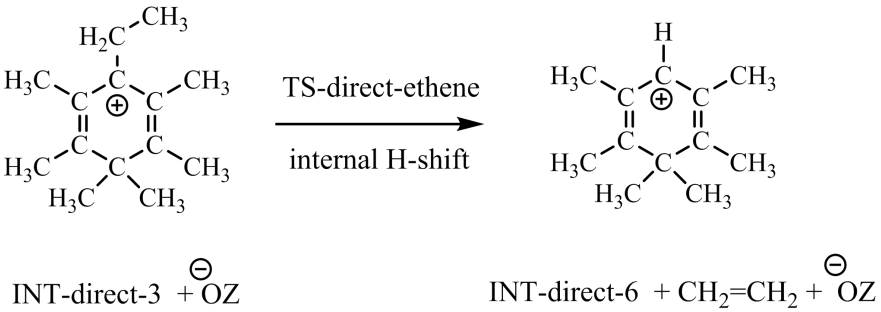

Scheme S1 The proposed pathway for the formation of ethene in phosphorus modified H-FAU zeolite.

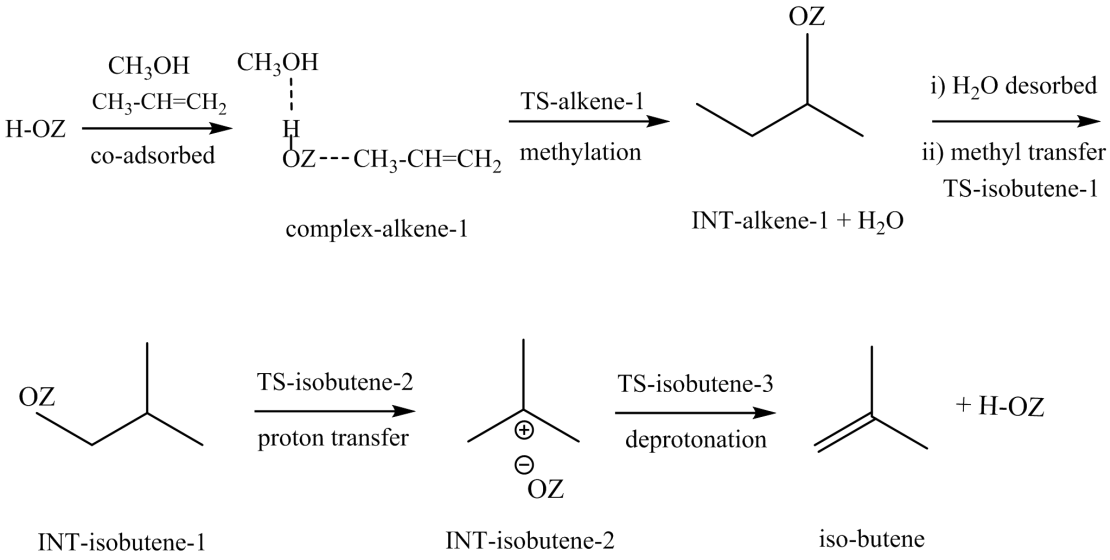

Scheme S2 The proposed pathway for the formation of iso-butene in phosphorus modified H-FAU zeolite.

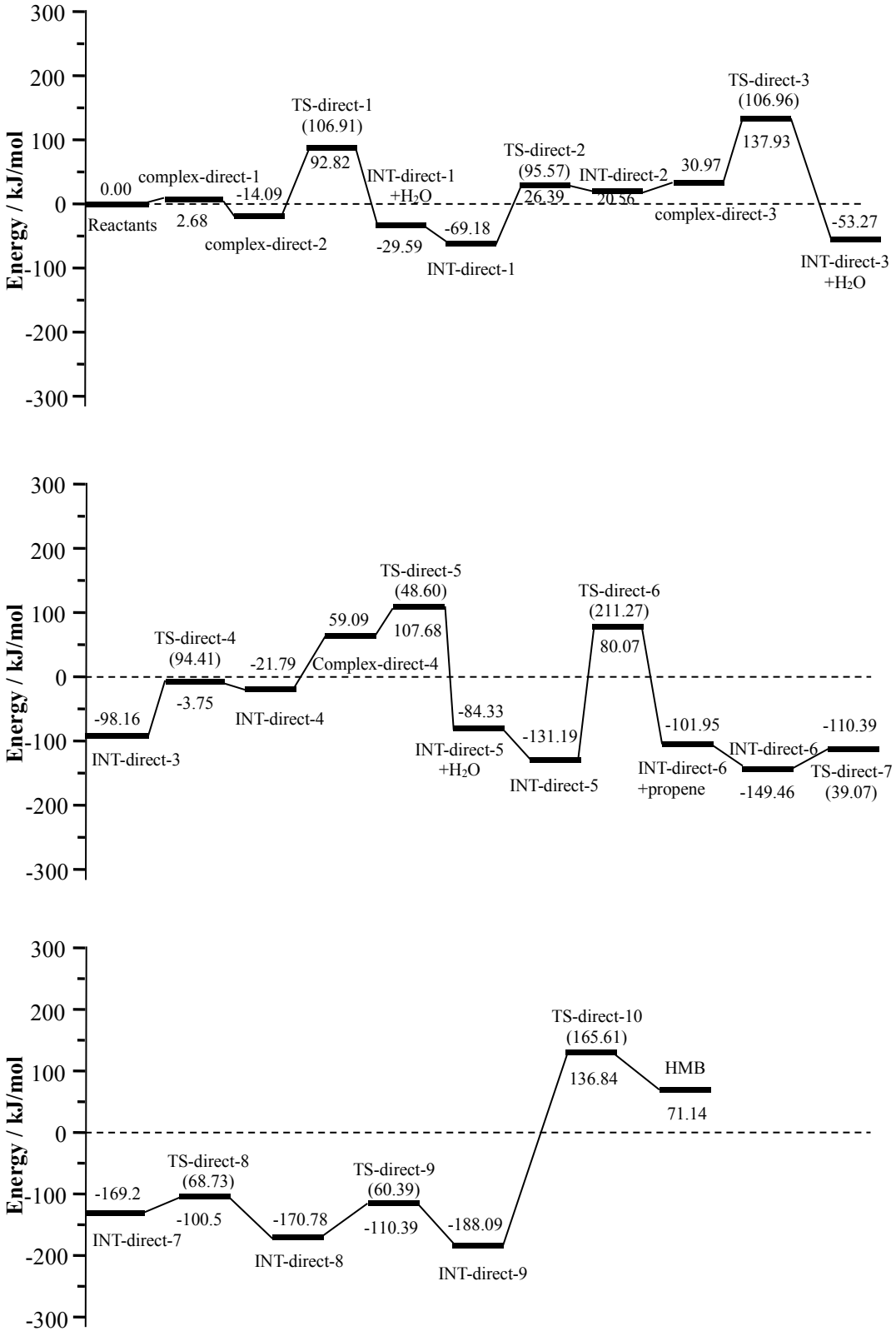

Fig. S1 Free energy profiles calculated for the direct internal H-shift pathway illustrated in Scheme 1 over phosphorus modified FAU zeolite at 673.15 K. The zeolite framework, the methanol and H_2O in the gaseous phase at infinite separation are taken as the reference state. For transition states, the activation barriers are given in parentheses.

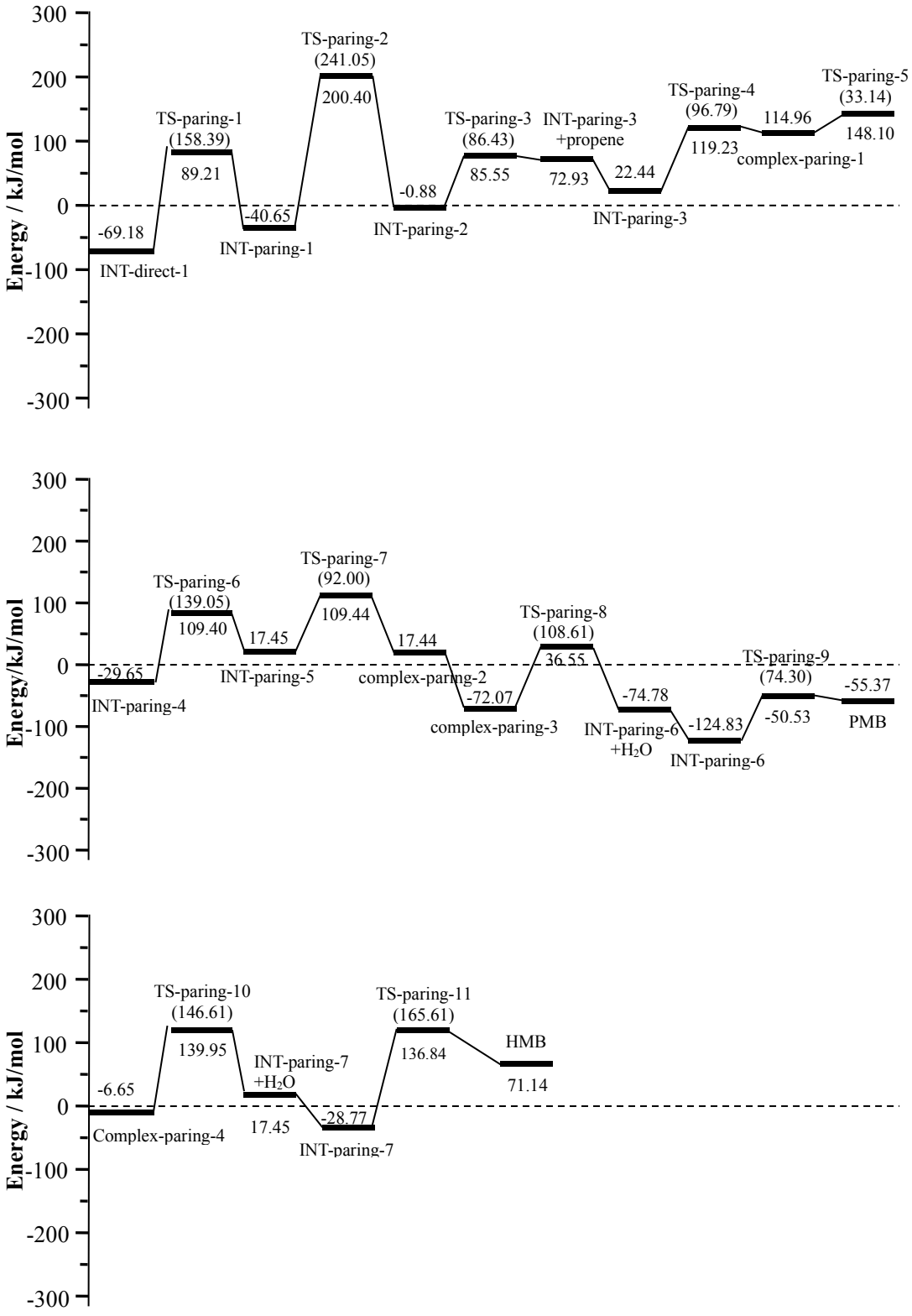

Fig. S2 Free energy profiles calculated for the paring pathway illustrated in Scheme 2 over phosphorus modified FAU zeolite at 673.15 K. The zeolite framework, methanol and H_2O in the gaseous phase at infinite separation are taken as the reference state. For transition states, the activation barriers are given in parentheses. For simplicity, the same steps (from reactants to INT-direct-1 in Scheme 1) are omitted.

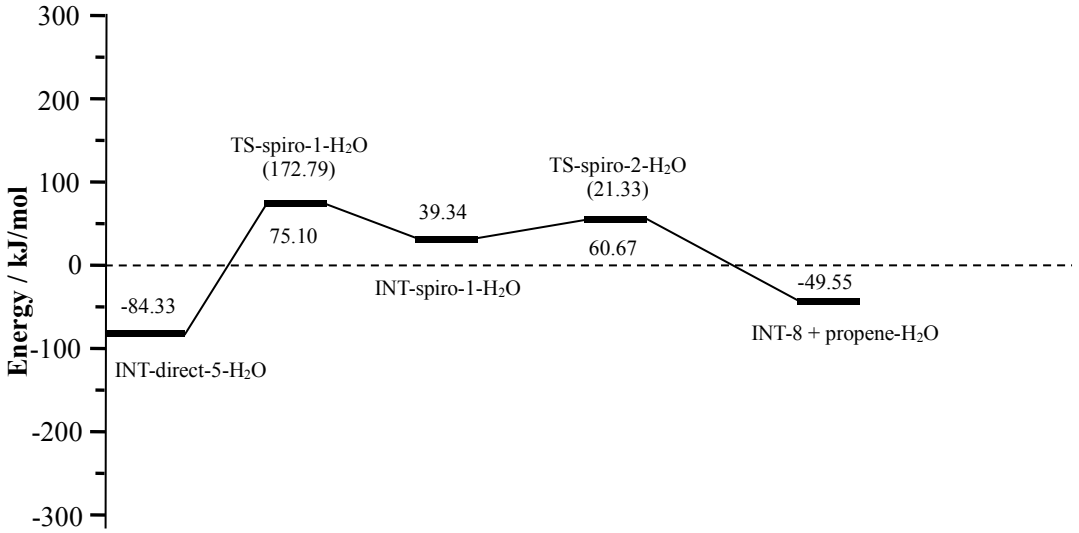

(a)

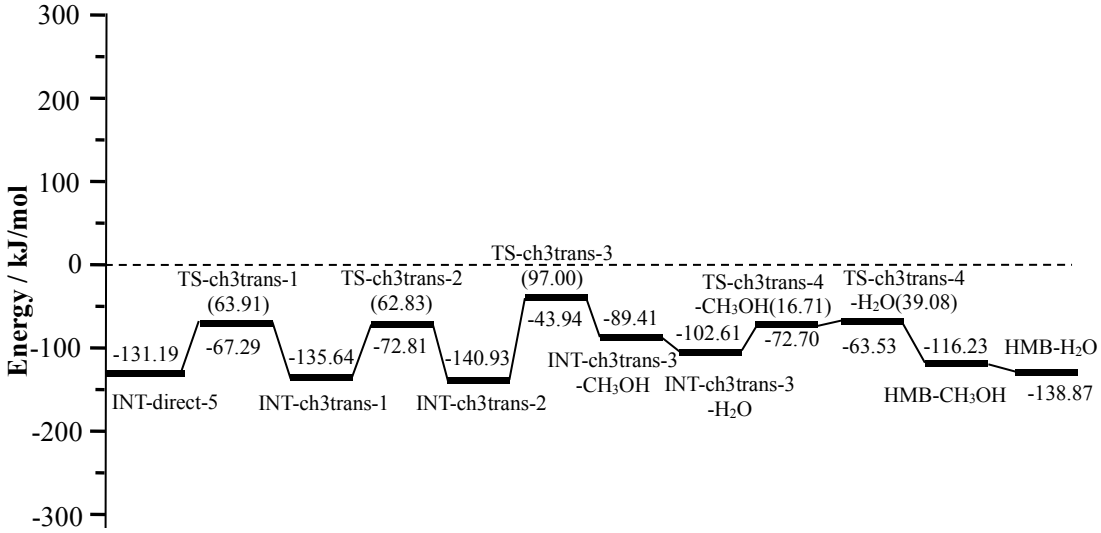

(b)

Fig. S3 Free energy profiles calculated for the indirect spiro (a) and methyl-transfer (b) pathways illustrated in Scheme 3 over phosphorus modified FAU zeolite at 673.15 K. The zeolite framework, methanol and H_2O in the gaseous phase at infinite separation are taken as the reference state. For transition states, the activation barriers are given in parentheses. For simplicity, the same steps (from reactants to INT-direct-5 in Scheme 1) are omitted.

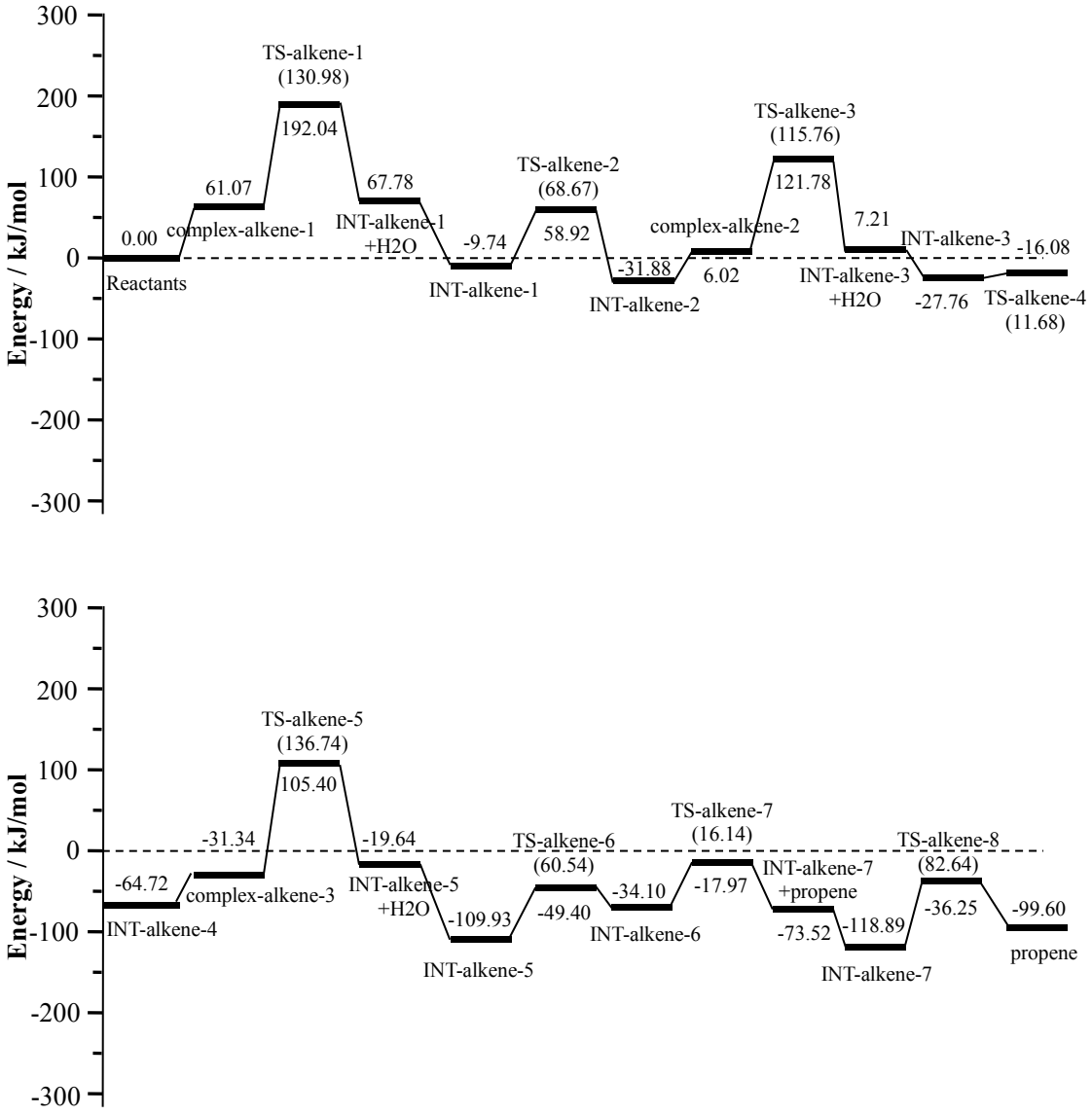

Fig. S4 Free energy profiles calculated for the formation of propene via the alkene cycle illustrated in Scheme 4 over phosphorus modified FAU zeolite at 673.15 K. The zeolite framework, methanol, propene, and H_2O in the gaseous phase at infinite separation are taken as the reference state. For transition states, the activation barriers are given in parentheses.

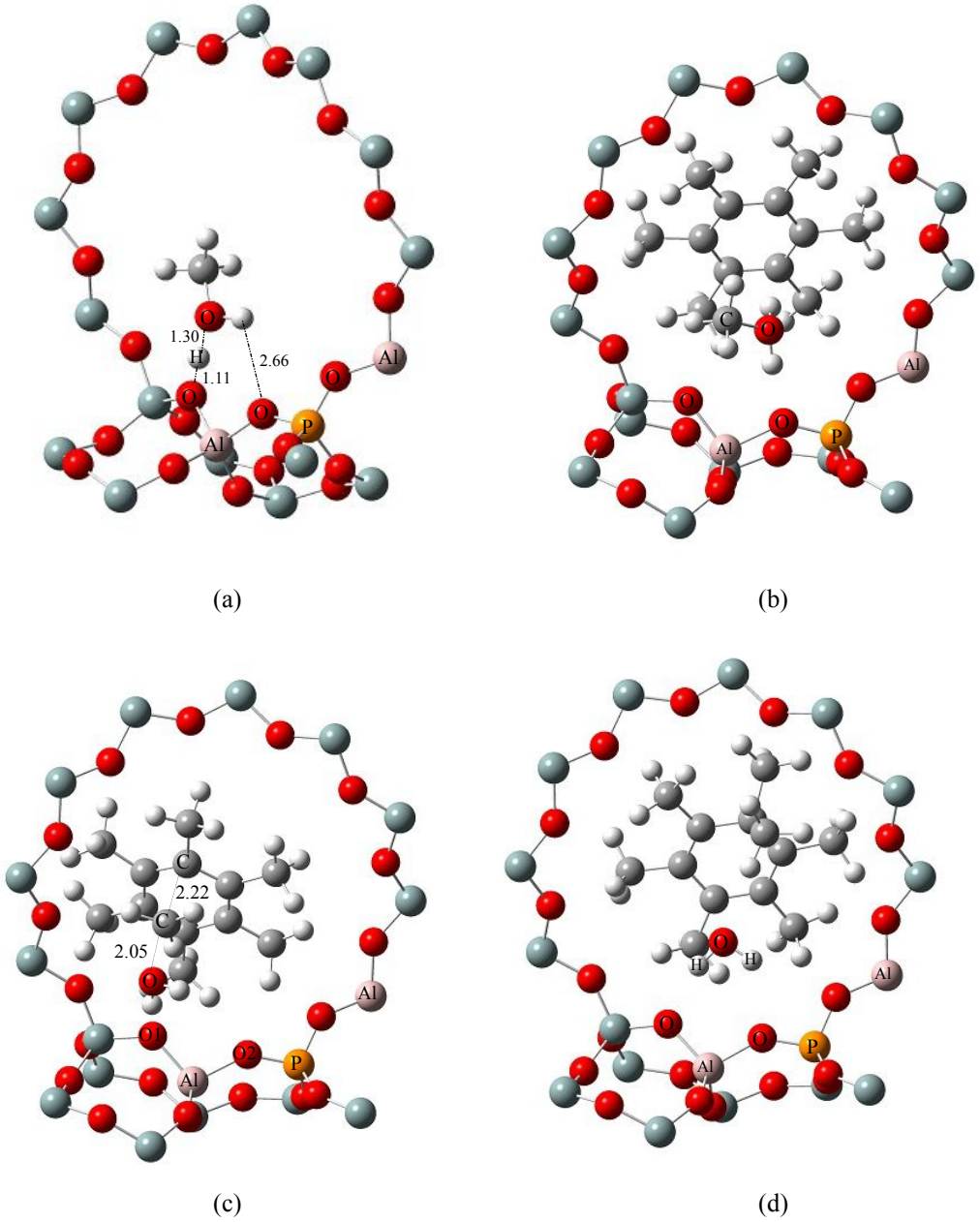

(a) (b)

(c) (d)

Fig. S5 Optimized structures of (a) complex-direct-1, (b) complex-direct-2, (c) TS-direct-1, and (d) INT-direct-1.

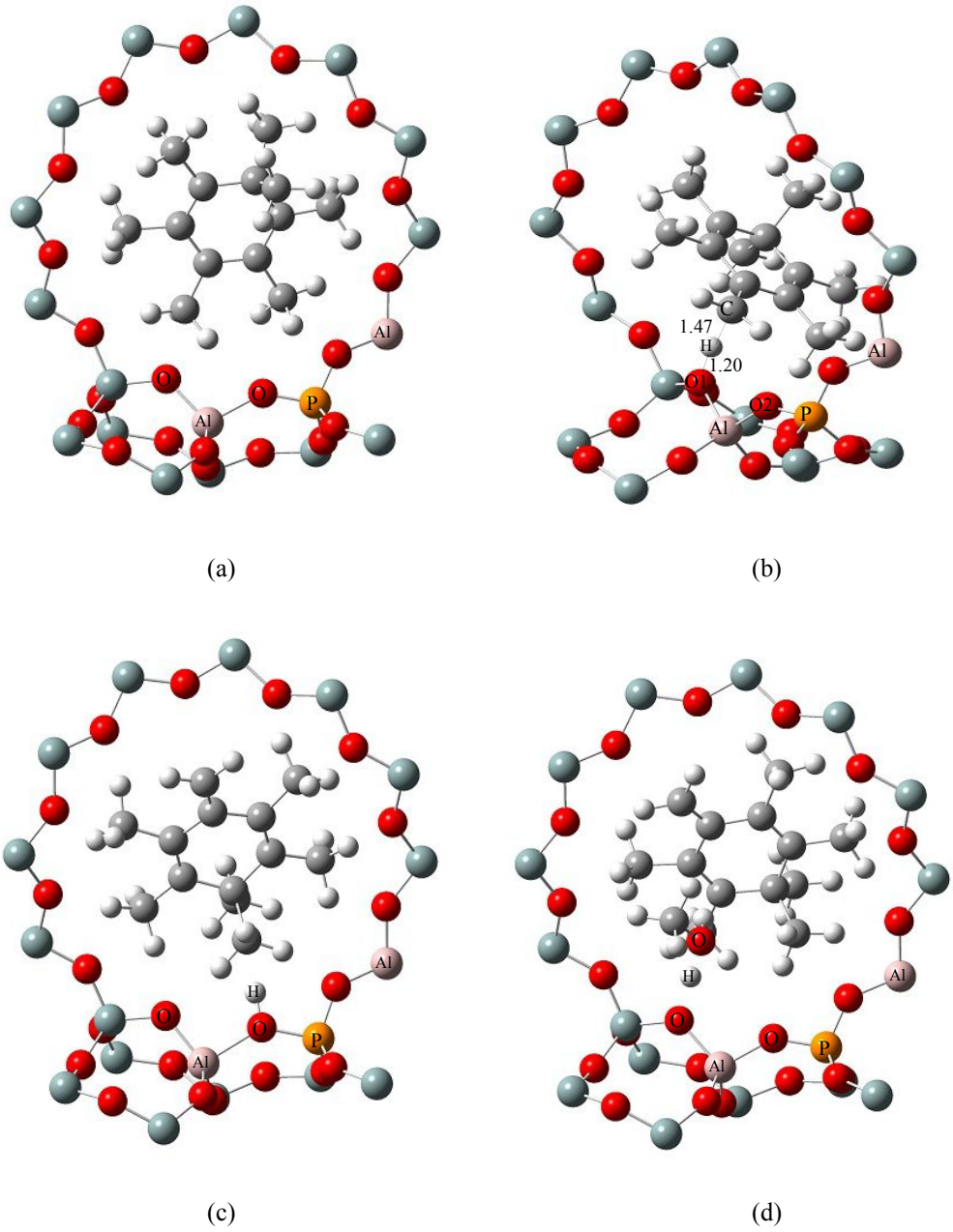

(a) (b)

(c) (d)

Fig. S6 Optimized structures of (a) INT-direct-1-noH_2O, (b) TS-direct-2, (c) INT-direct-2, and (d) complex-direct-3.

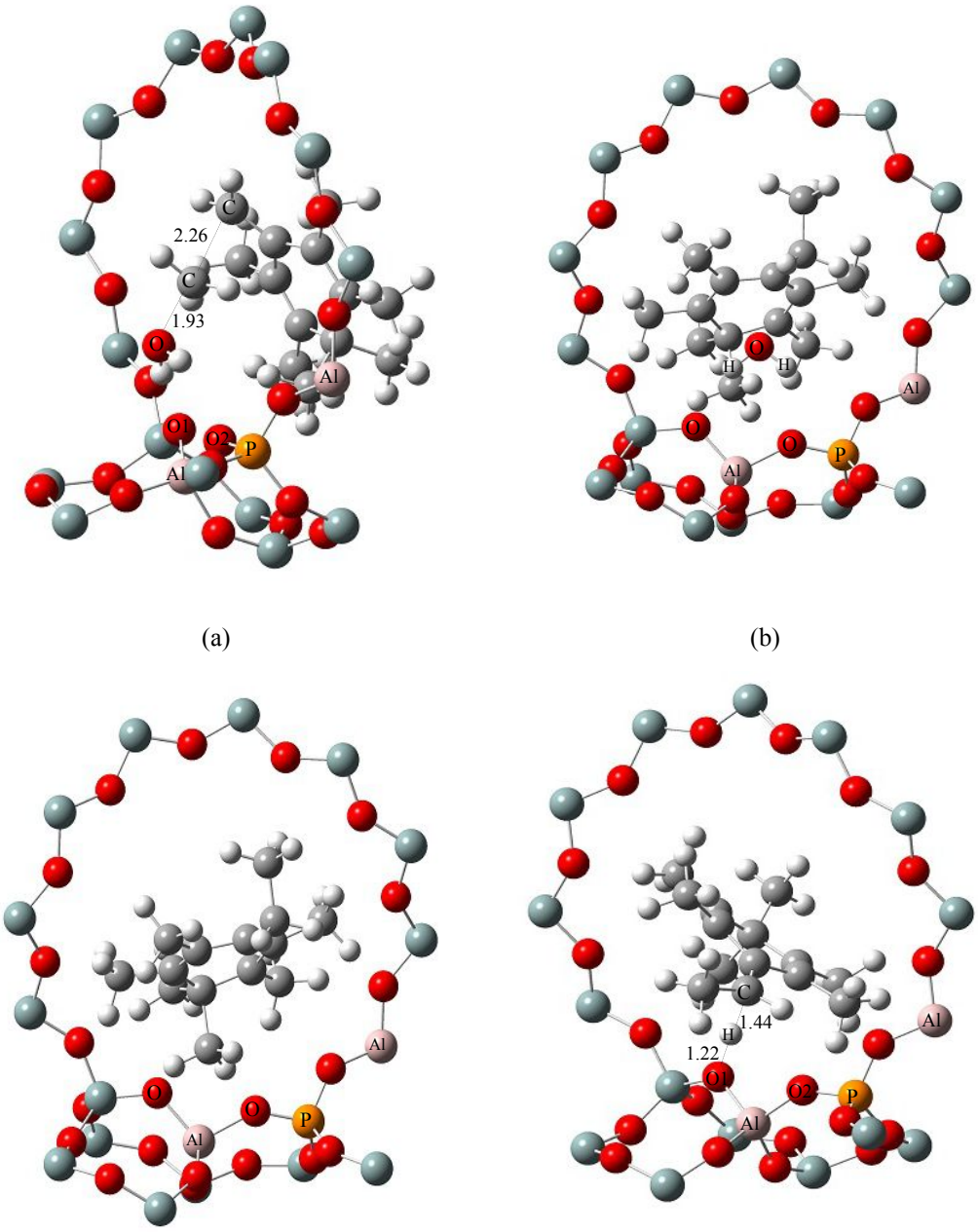

Fig. S7 Optimized structures of (a) TS-direct-3, (b) INT-direct-3, (c) INT-direct-3-noH_2O, and (d) TS-direct-4.

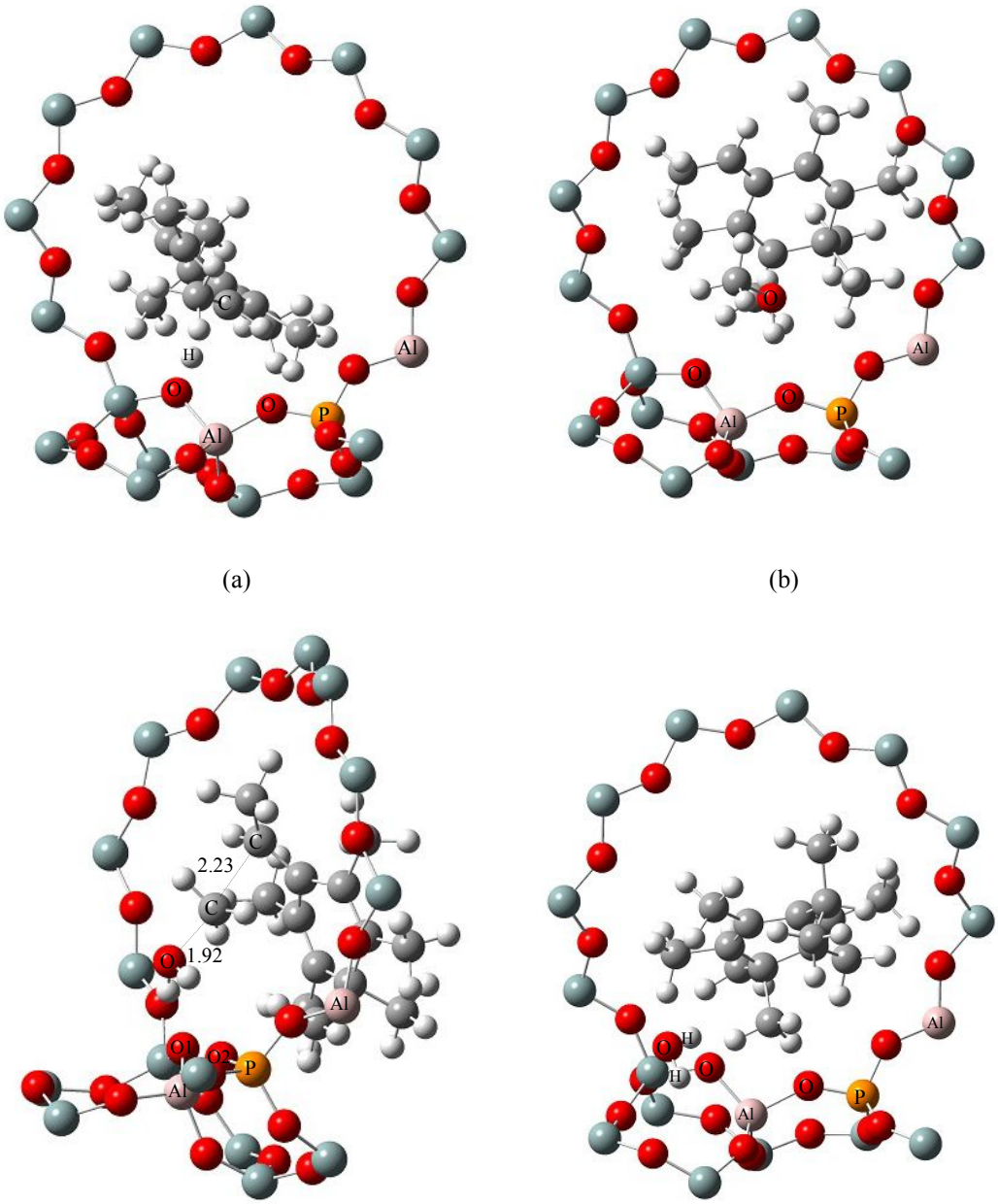

Fig. S8 Optimized structures of (a) INT-direct-4, (b) complex-direct-4, (c) TS-direct-5, and (d) INT-direct-5.

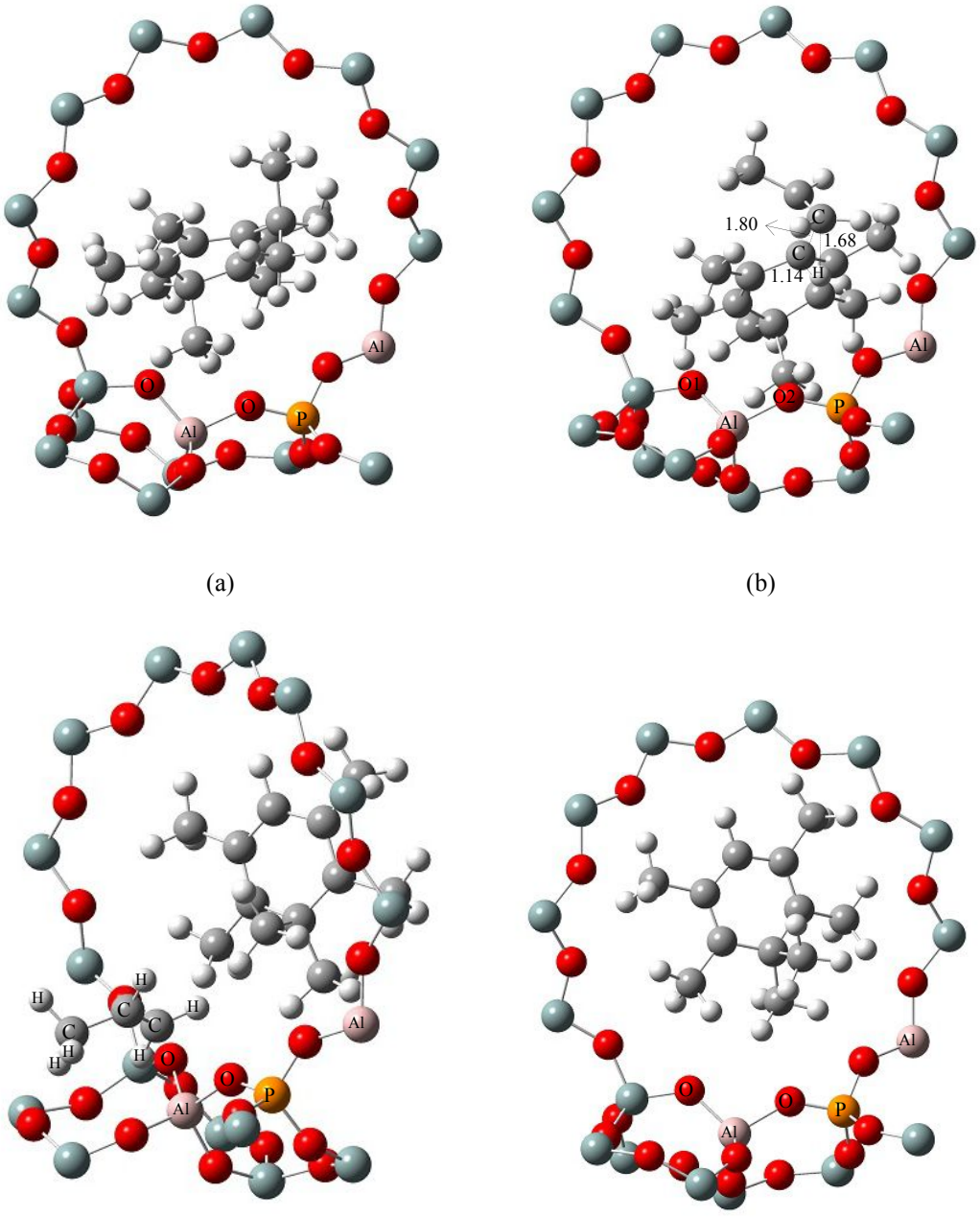

Fig. S9 Optimized structures of (a) INT-direct-5-noH_2O, (b) TS-direct-6, (c) INT-direct-6, and (d) INT-direct-6-nopropene.

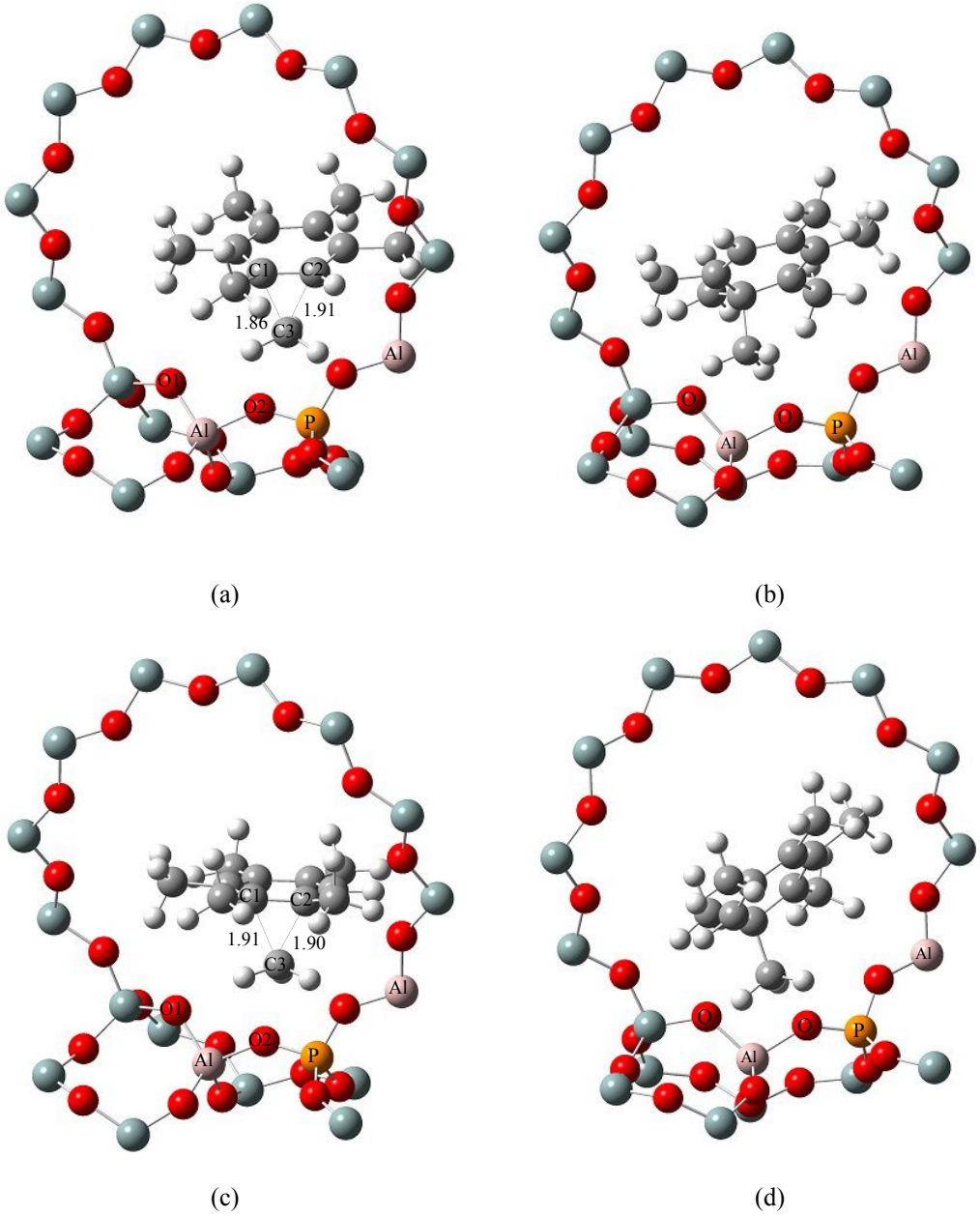

Fig. S10 Optimized structures of (a) TS-direct-7, (b) INT-direct-7, (c) TS-direct-8, and (d) INT-direct-8.

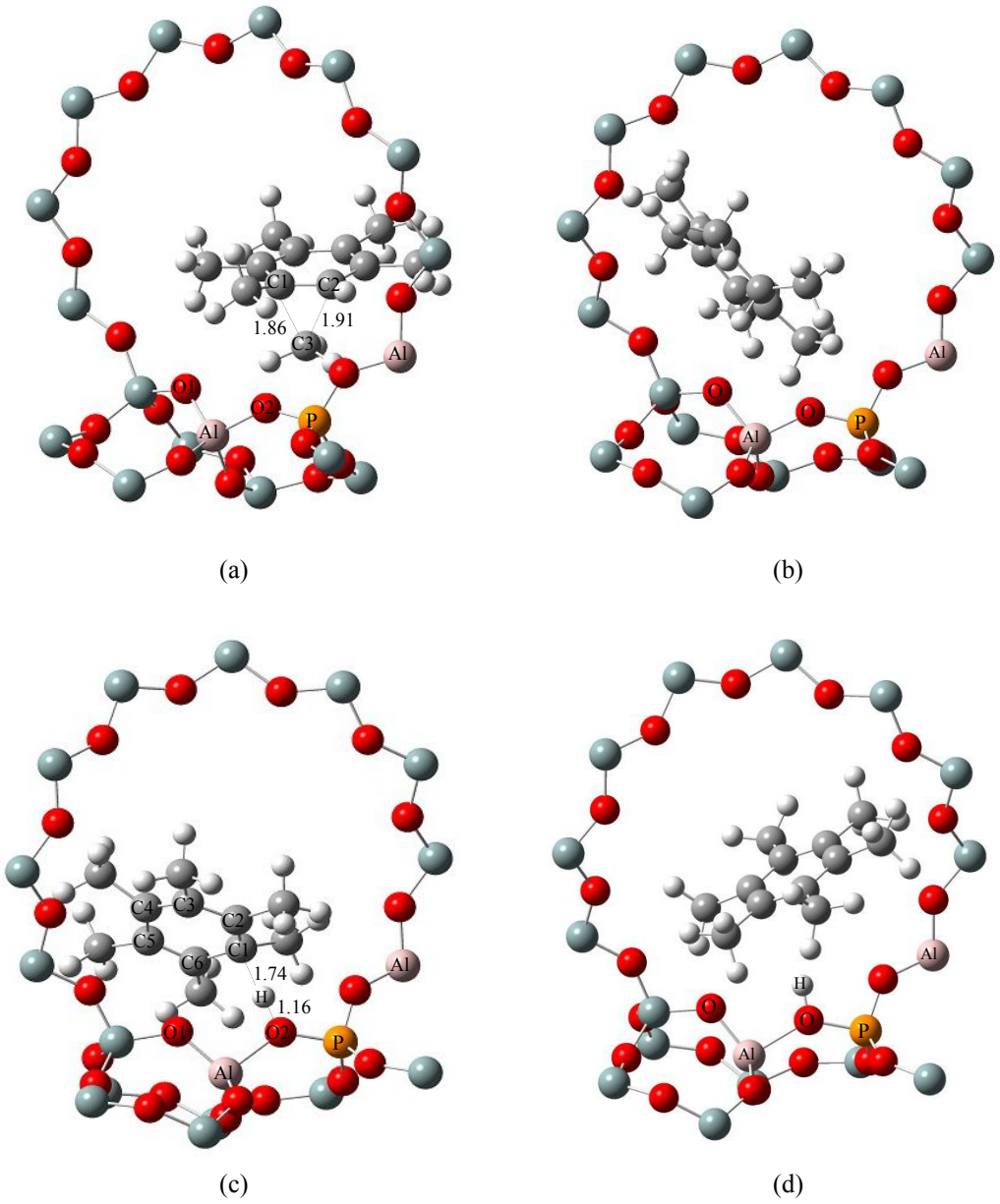

Fig. S11 Optimized structures of (a) TS-direct-9, (b) INT-direct-9, (c) TS-direct-10, and (d) HMB.

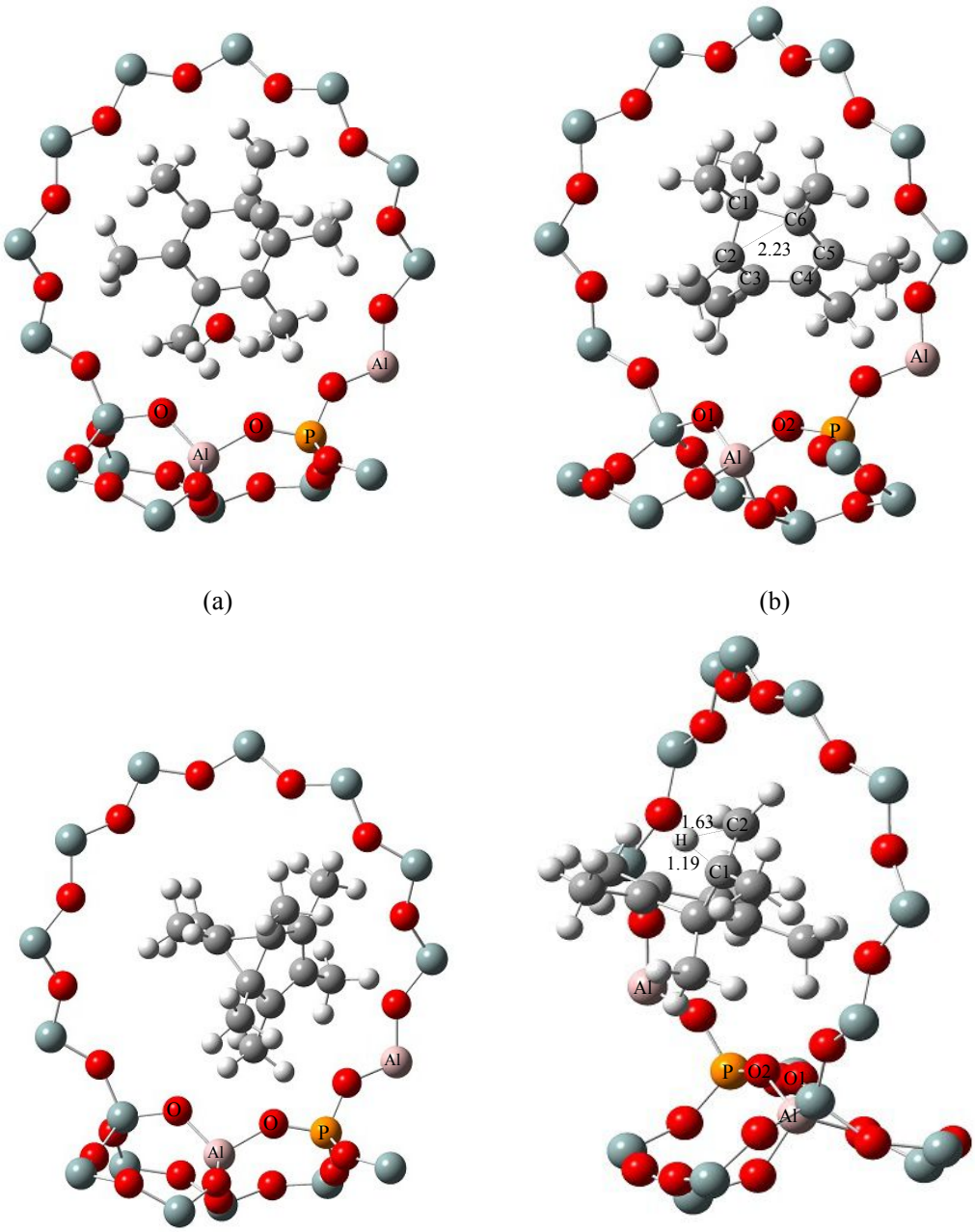

Fig. S12 Optimized structures of (a) INT-direct-1, (b) TS-paring-1, (c) INT-paring-1, and (d) TS-paring-2.

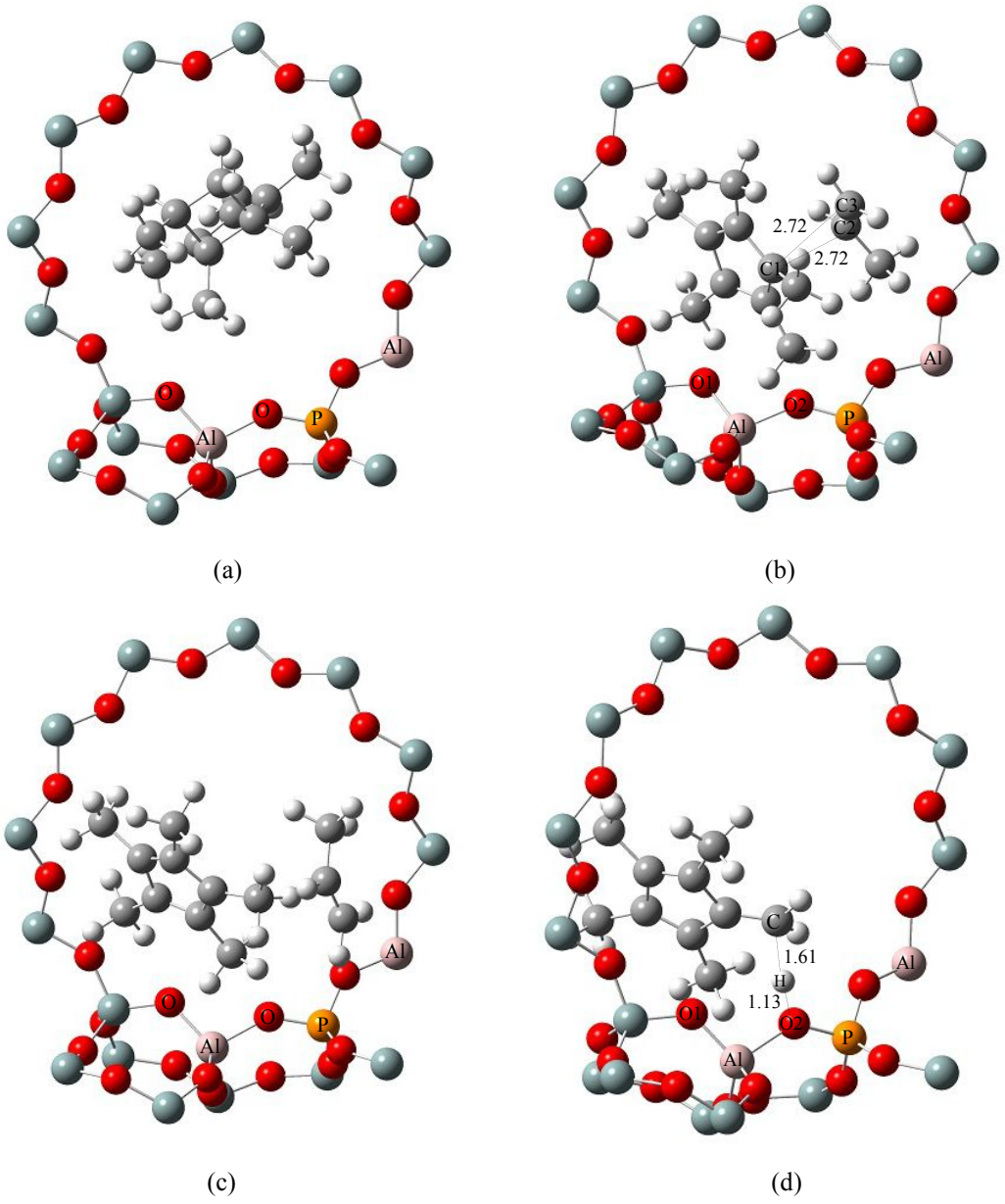

Fig. S13 Optimized structures of (a) INT-paring-2, (b) TS-paring-3, (c) INT-paring-3, and (d) TS-paring-4.

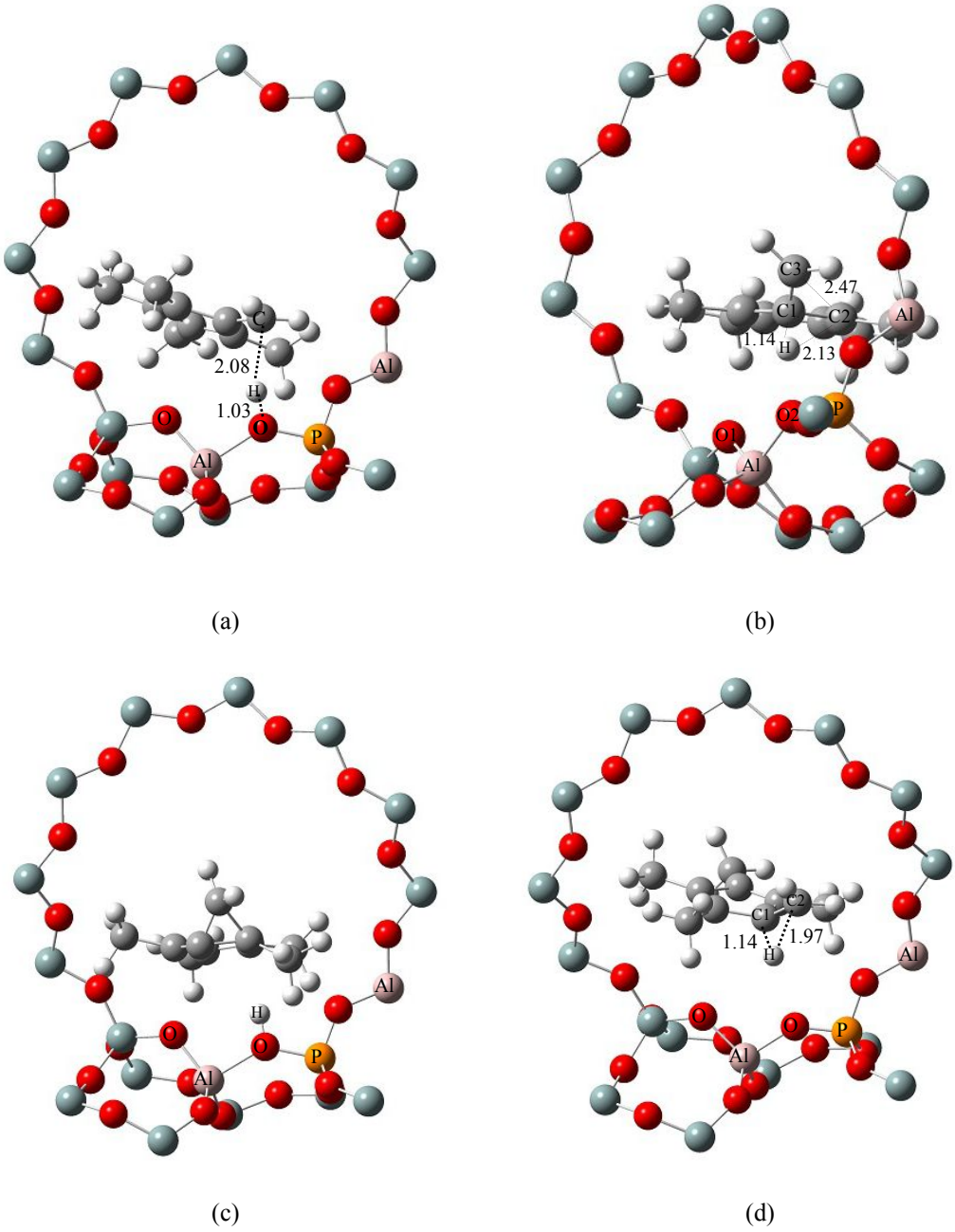

Fig. S14 Optimized structures of (a) complex-paring-1, (b) TS-paring-5, (c) INT-paring-4, and (d) TS-paring-6.

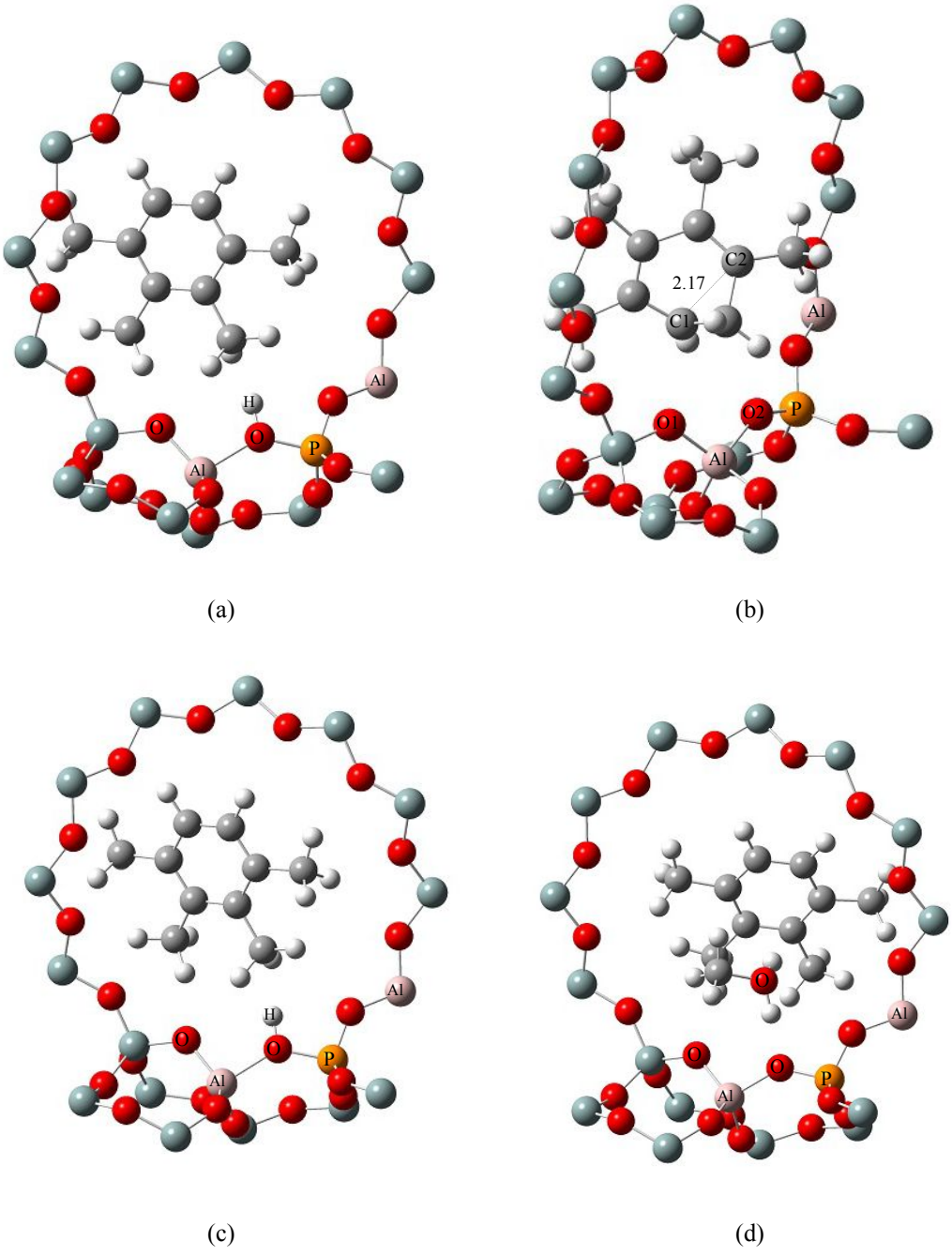

Fig. S15 Optimized structures of (a) INT-paring-5, (b) TS-paring-7, (c) complex-paring-2, and (d) complex-paring-3.

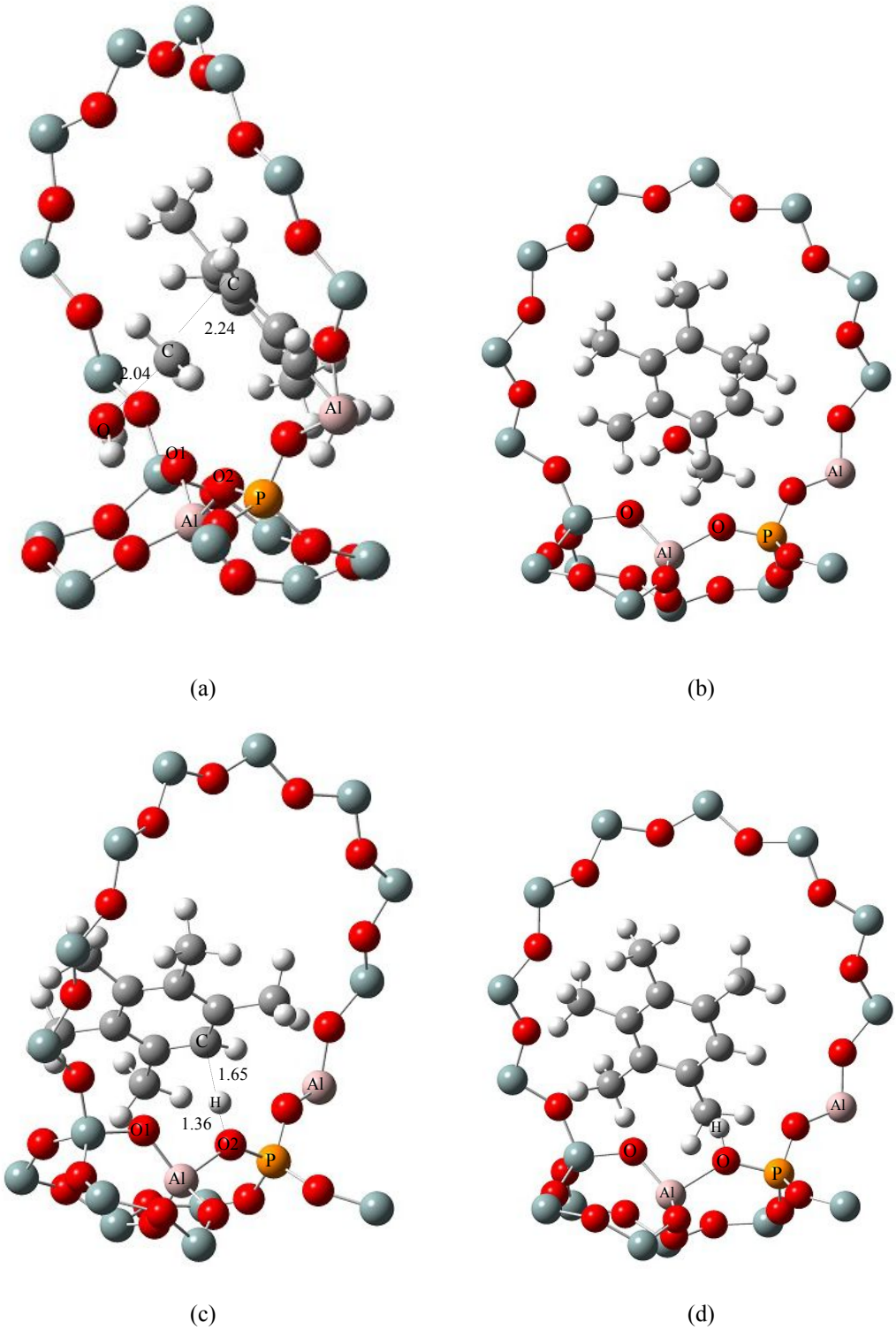

Fig. S16 Optimized structures of (a) TS-paring-8, (b) INT-paring-6, (c) TS-paring-9, and (d) PMB.

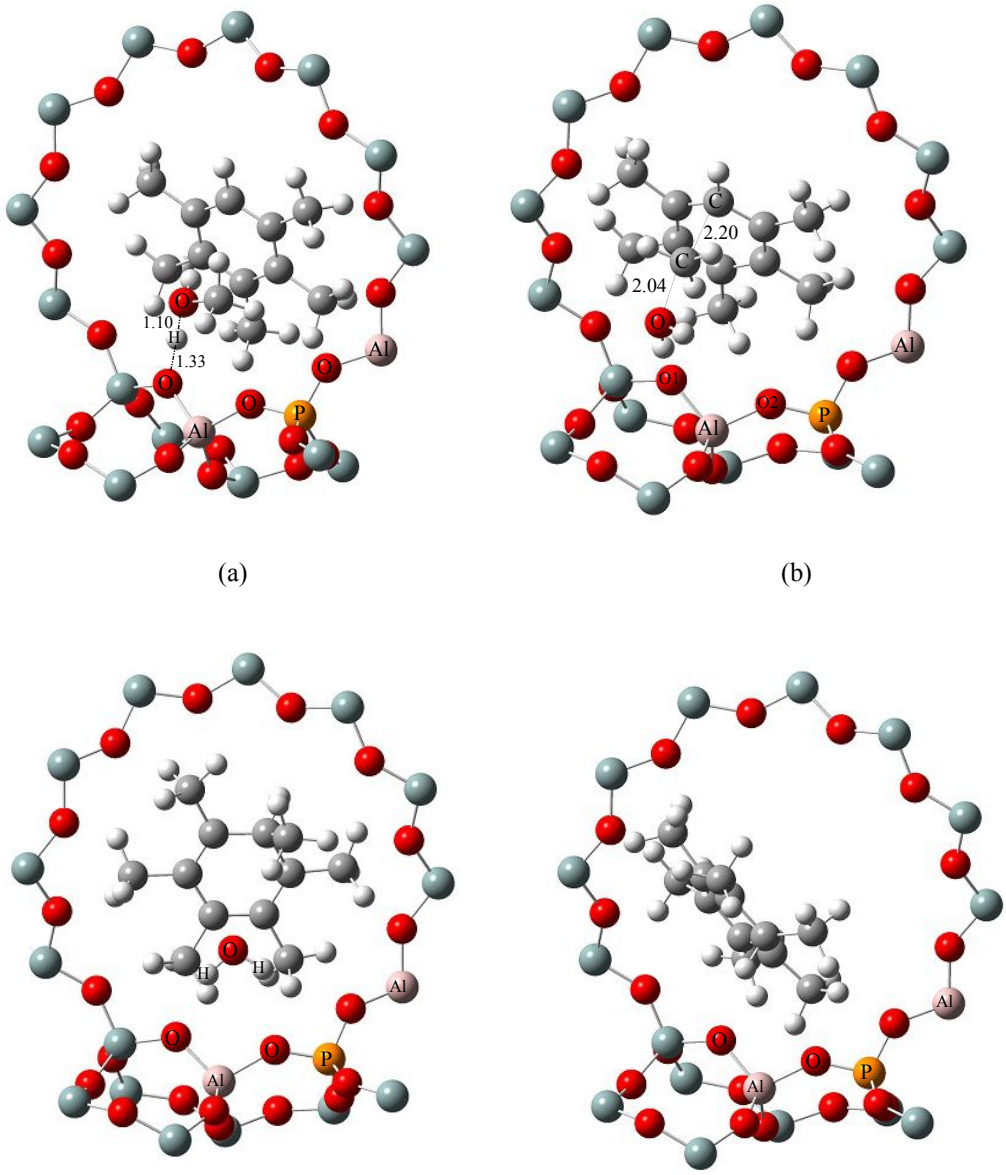

Fig. S17 Optimized structures of (a) complex-paring-4, (b) TS-paring-10, (c) INT-paring-7, and (d) INT-paring-7-noH_2O.

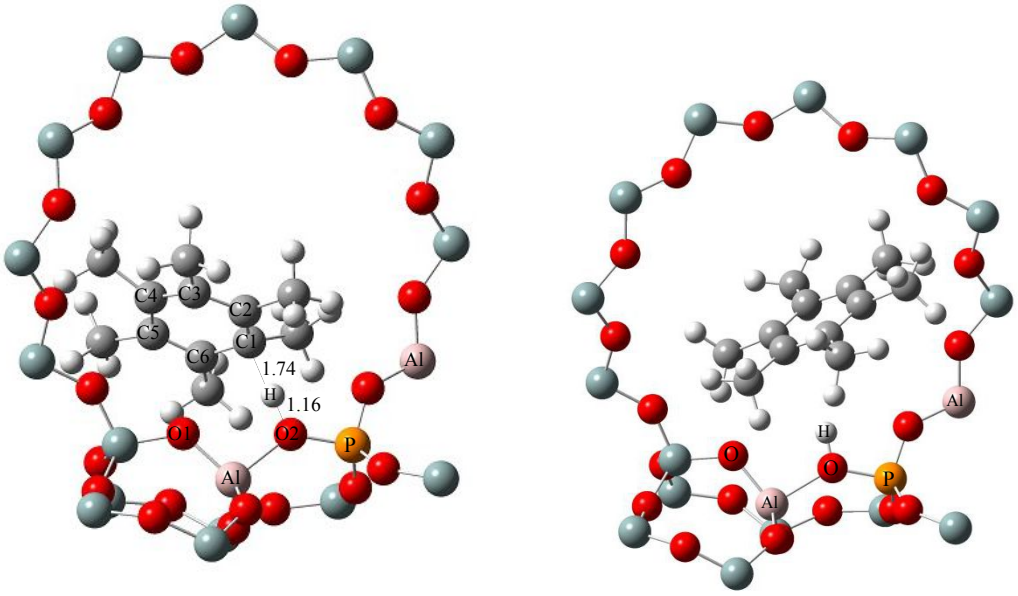

(a) (b)

Fig. S18 Optimized structures of (a) TS-paring-11, and (b) HMB.

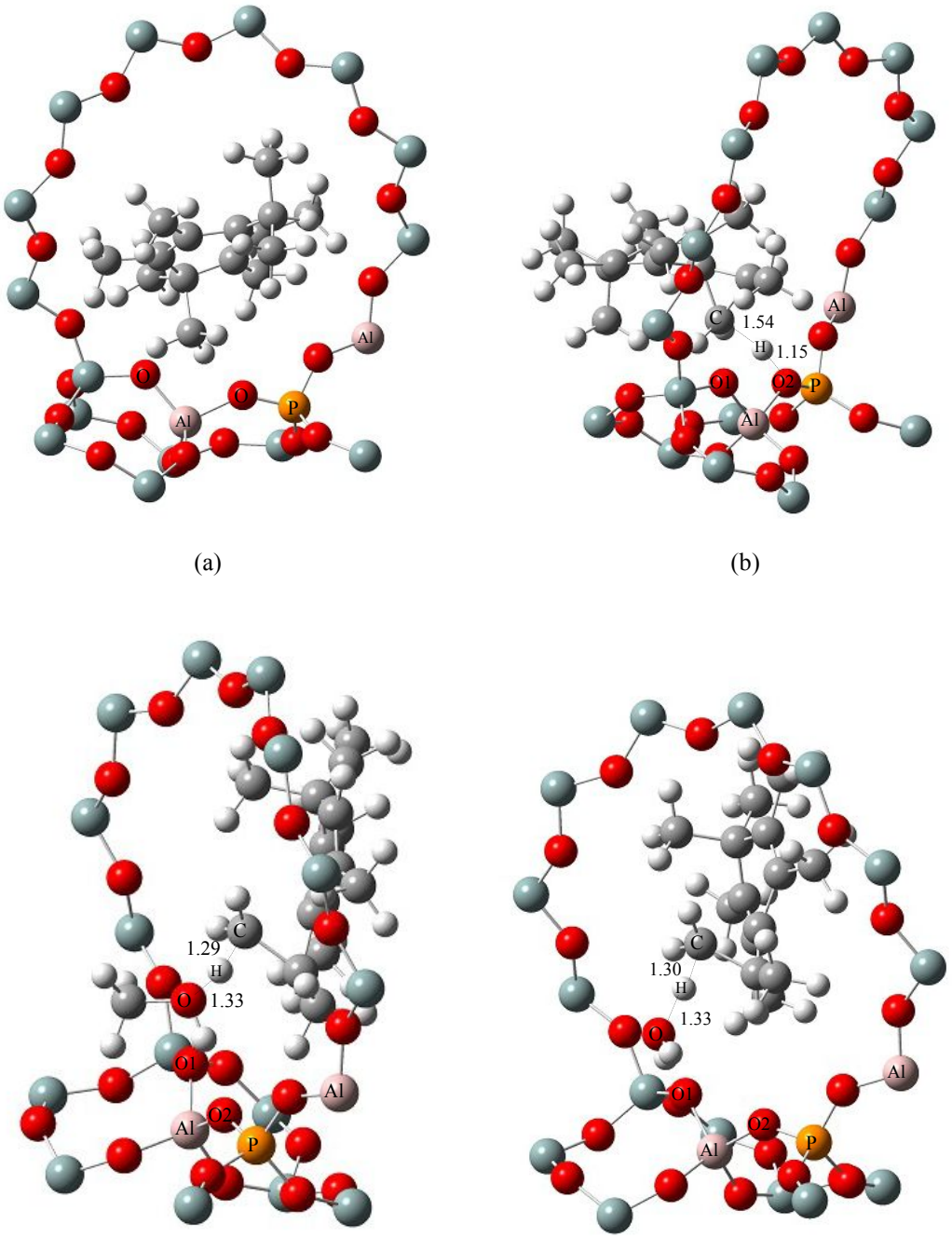

Fig. S19 Optimized structures of (a) INT-direct-5-noH_2O, (b) TS-spiro-1, (c) TS-spiro-1-CH_3OH, and (d) TS-spiro-1-H_2O.

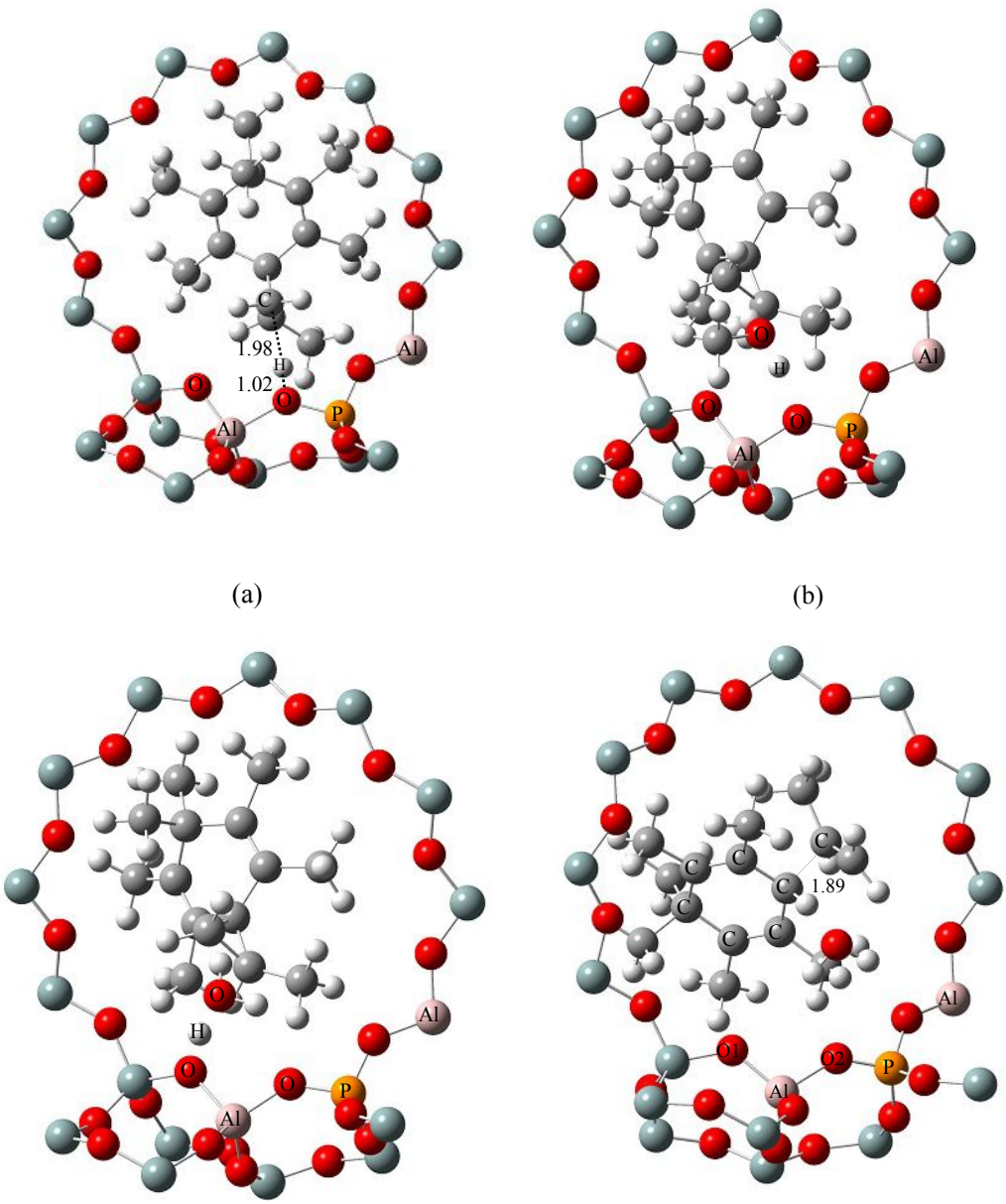

Fig. S20 Optimized structures of (a) INT-spiro-1, (b) INT-spiro-1-CH_3OH, (c) INT-spiro-1-H_2O, and (d) TS-spiro-2-H_2O.

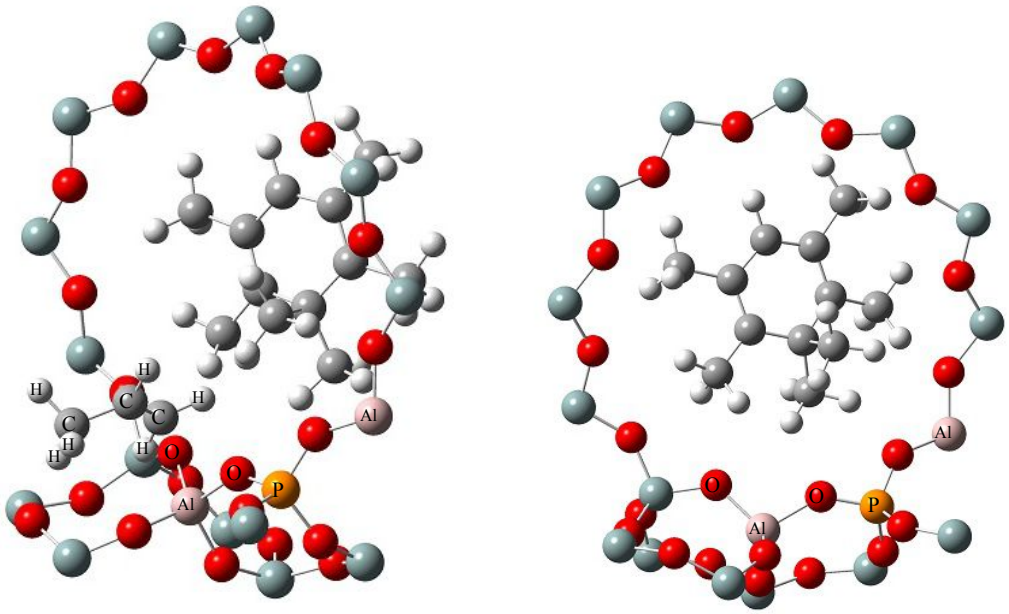

(a) (b)

Fig. S21 Optimized structures of (a) INT-direct-6, and (b) INT-direct-6-nopropene.

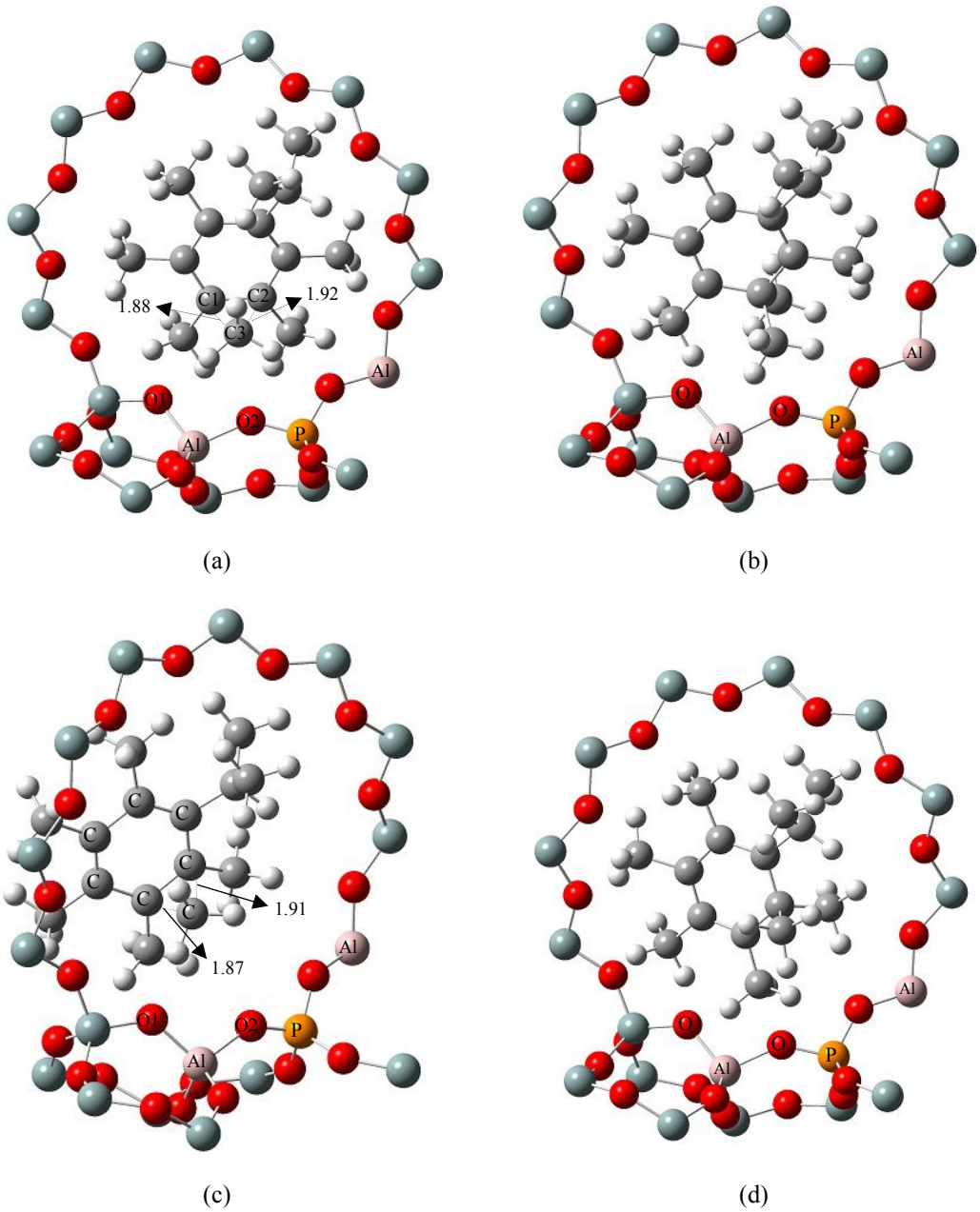

Fig. S22 Optimized structures of (a) TS-ch3trans-1, (b) INT-ch3trans-1, (c) TS-ch3trans-2, and (d) INT-ch3trans-2.

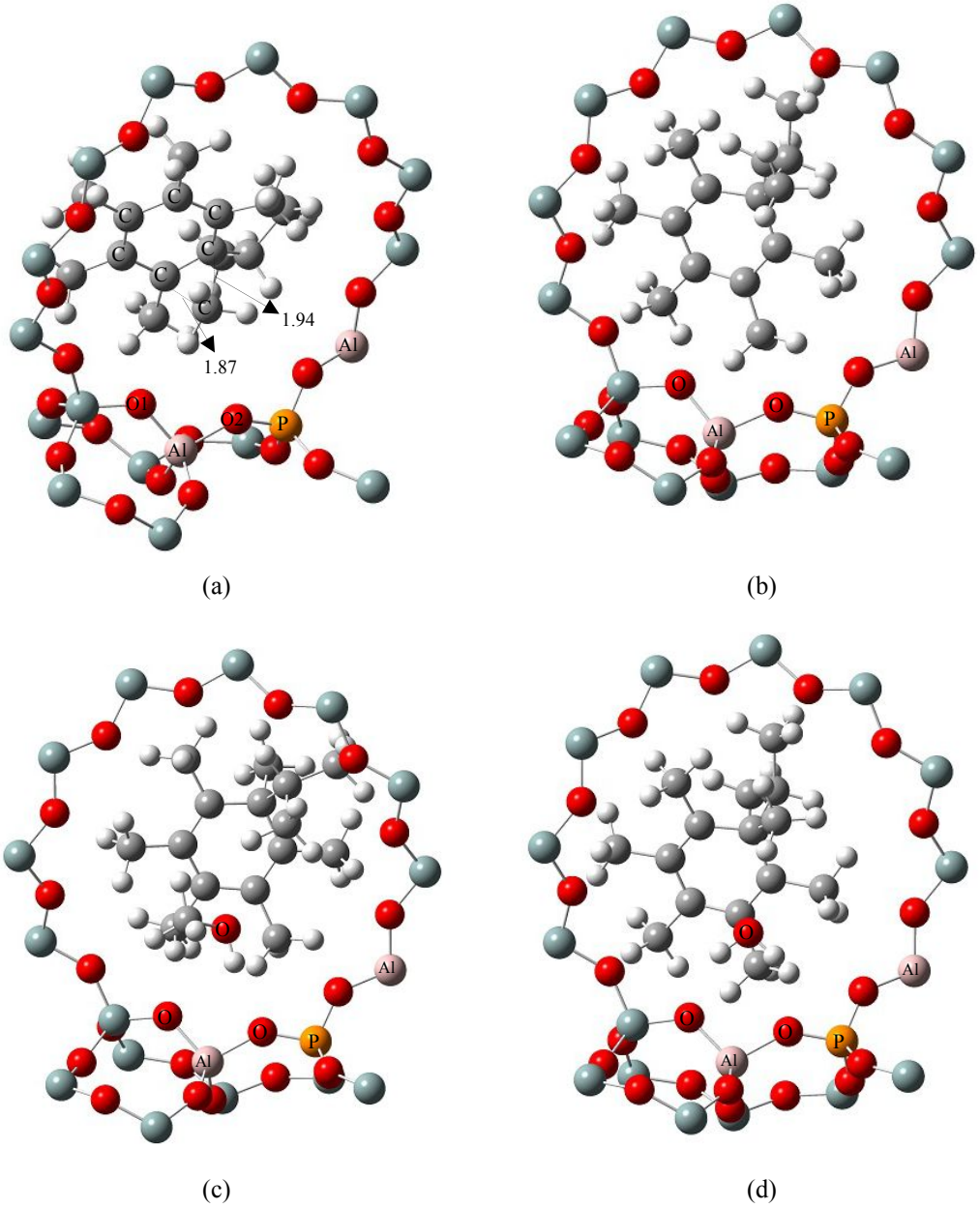

Fig. S23 Optimized structures of (a) TS-ch3trans-3, (b) INT-ch3trans-3, (c) INT-ch3trans-3-CH_3OH, and (d) INT-ch3trans-3-H_2O.

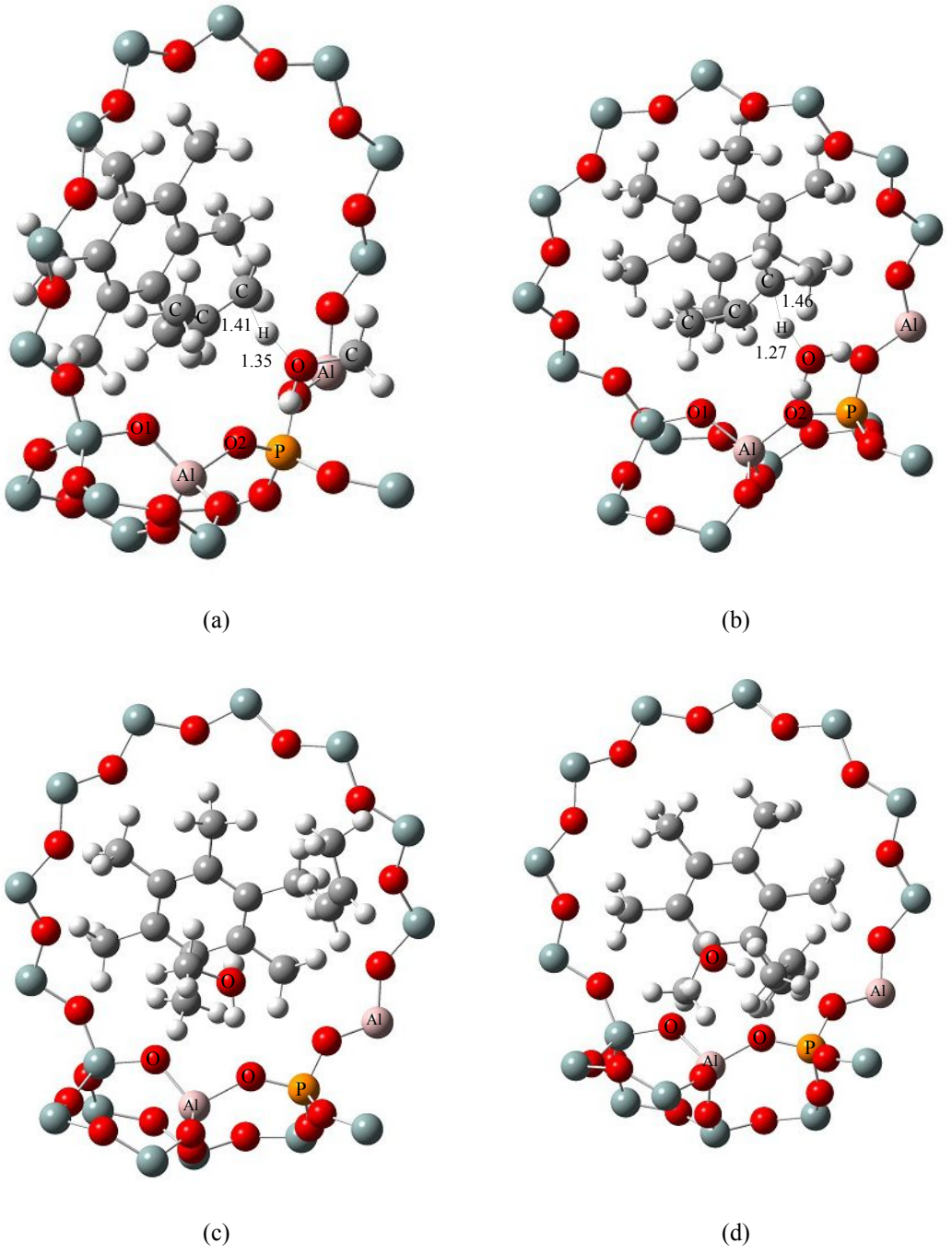

Fig. S24 Optimized structures of (a) TS-ch3trans-4-CH_3OH, (b) TS-ch3trans-4-H_2O, (c) HMB-CH_3OH, and (d) HMB-H_2O.

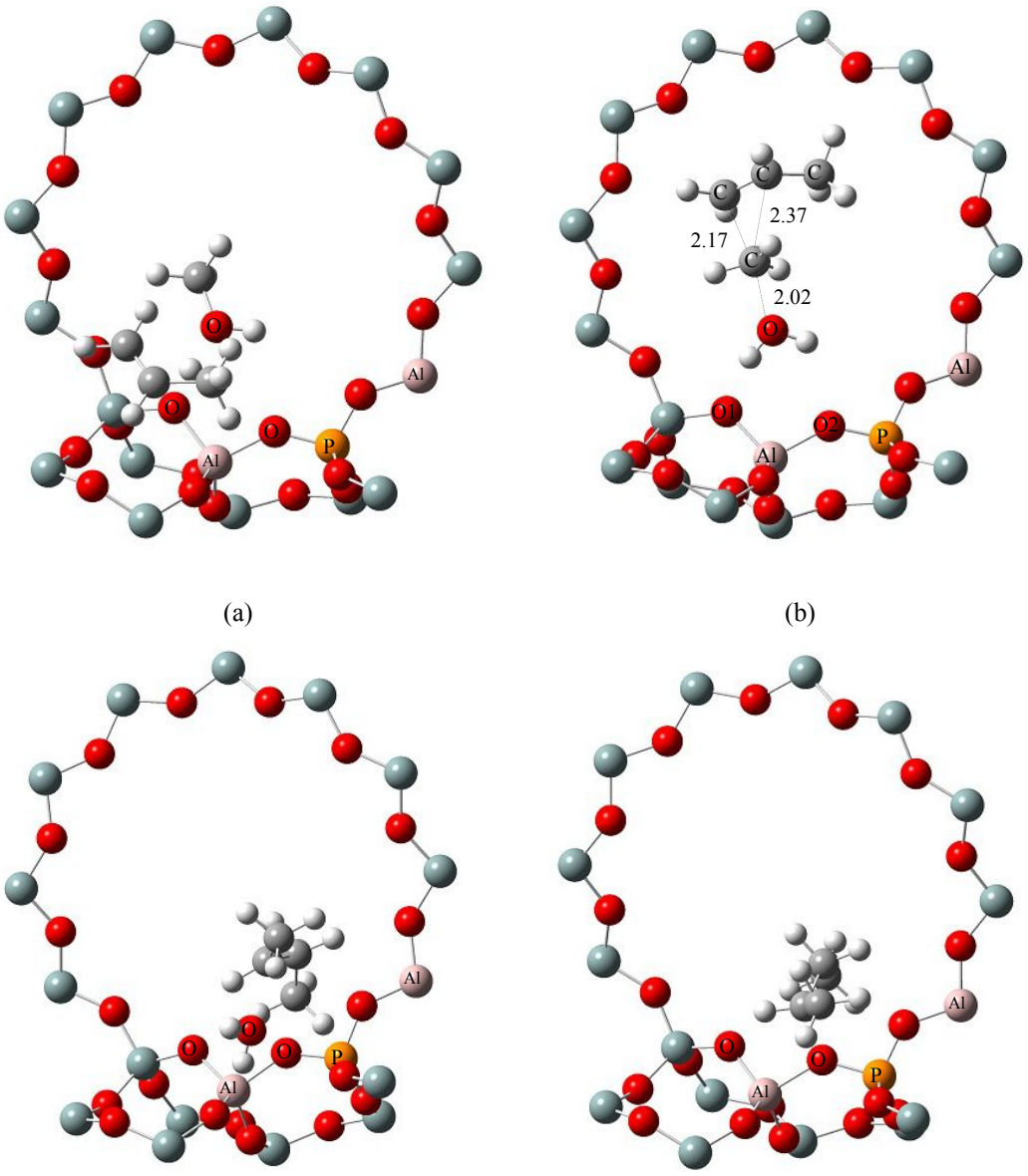

(a) (b)

(c) (d)

Fig. S25 Optimized structures of (a) complex-alkene-1, (b) TS-alkene-1, (c) INT-alkene-1, and (d) INT-alkene-noH_2O-1.

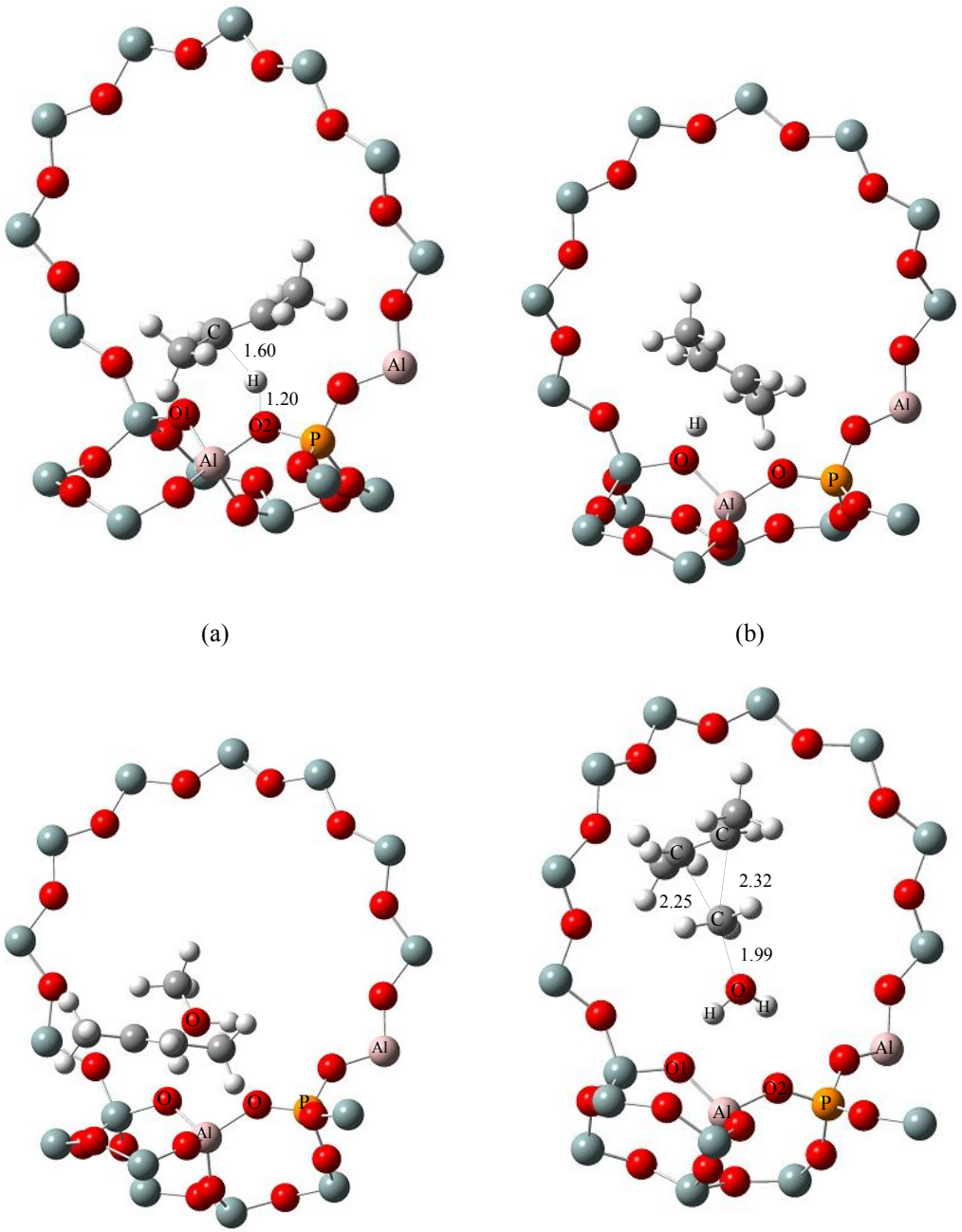

Fig. S26 Optimized structures of (a) TS-alkene-2, (b) INT-alkene-2, (c) complex-alkene-2, and (d) TS-alkene-3.

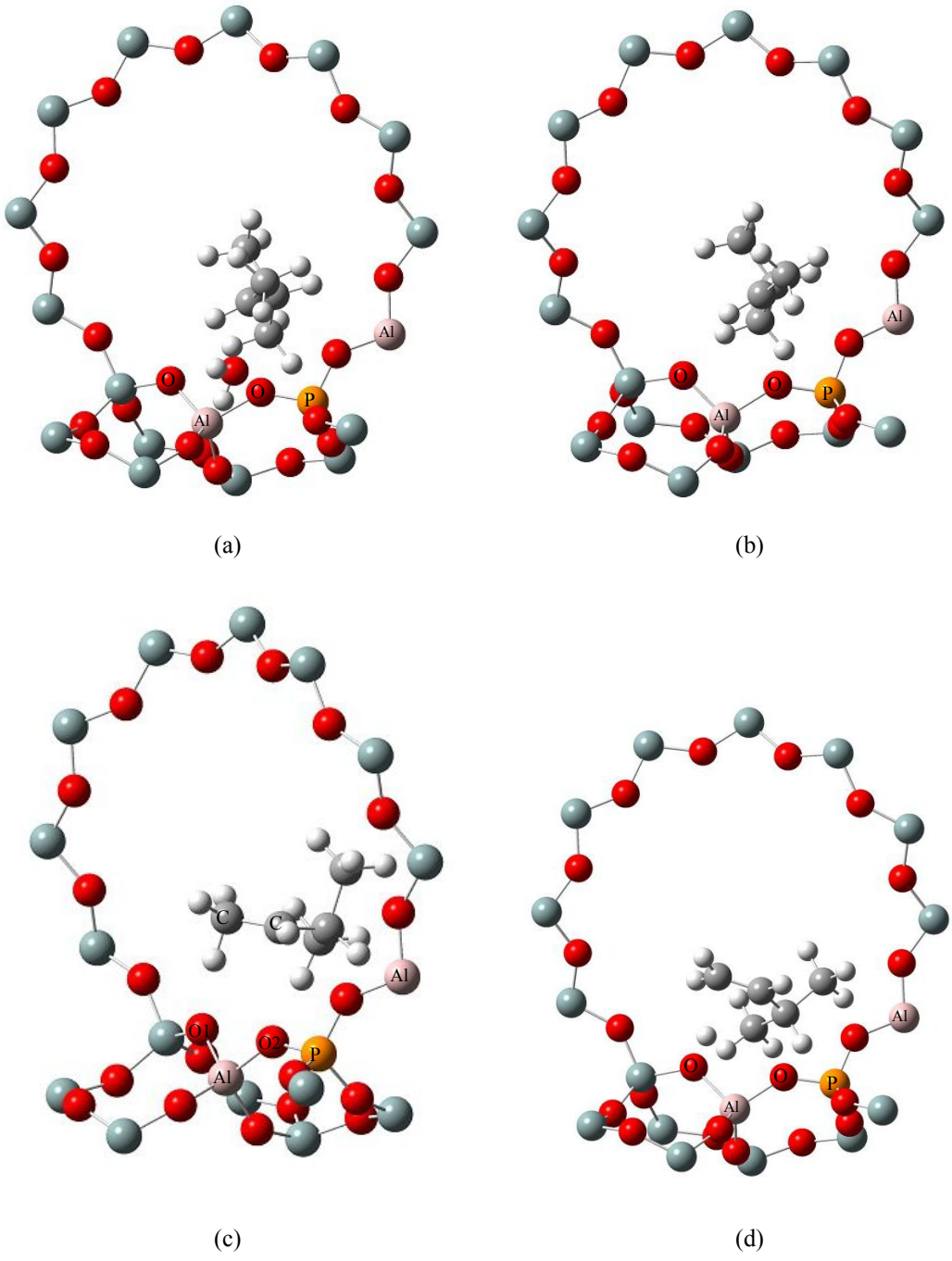

Fig. S27 Optimized structures of (a) INT-alkene-3, (b) INT-alkene-3-noH_2O, (c) TS-alkene-4, and (d) INT-alkene-4.

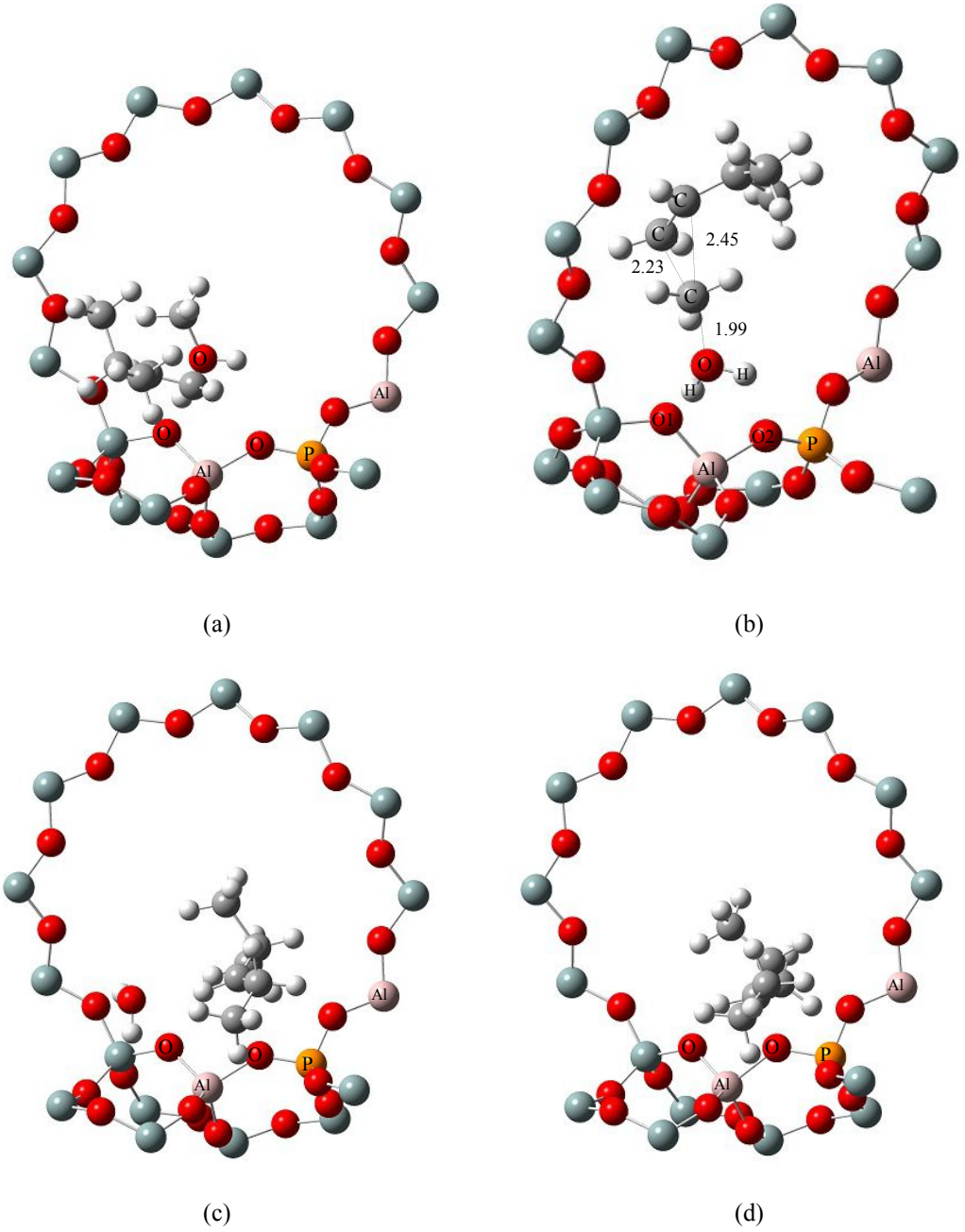

Fig. S28 Optimized structures of (a) complex-alkene-3, (b) TS-alkene-5, (c) INT-alkene-5, and (d) INT-alkene-5-noH_2O.

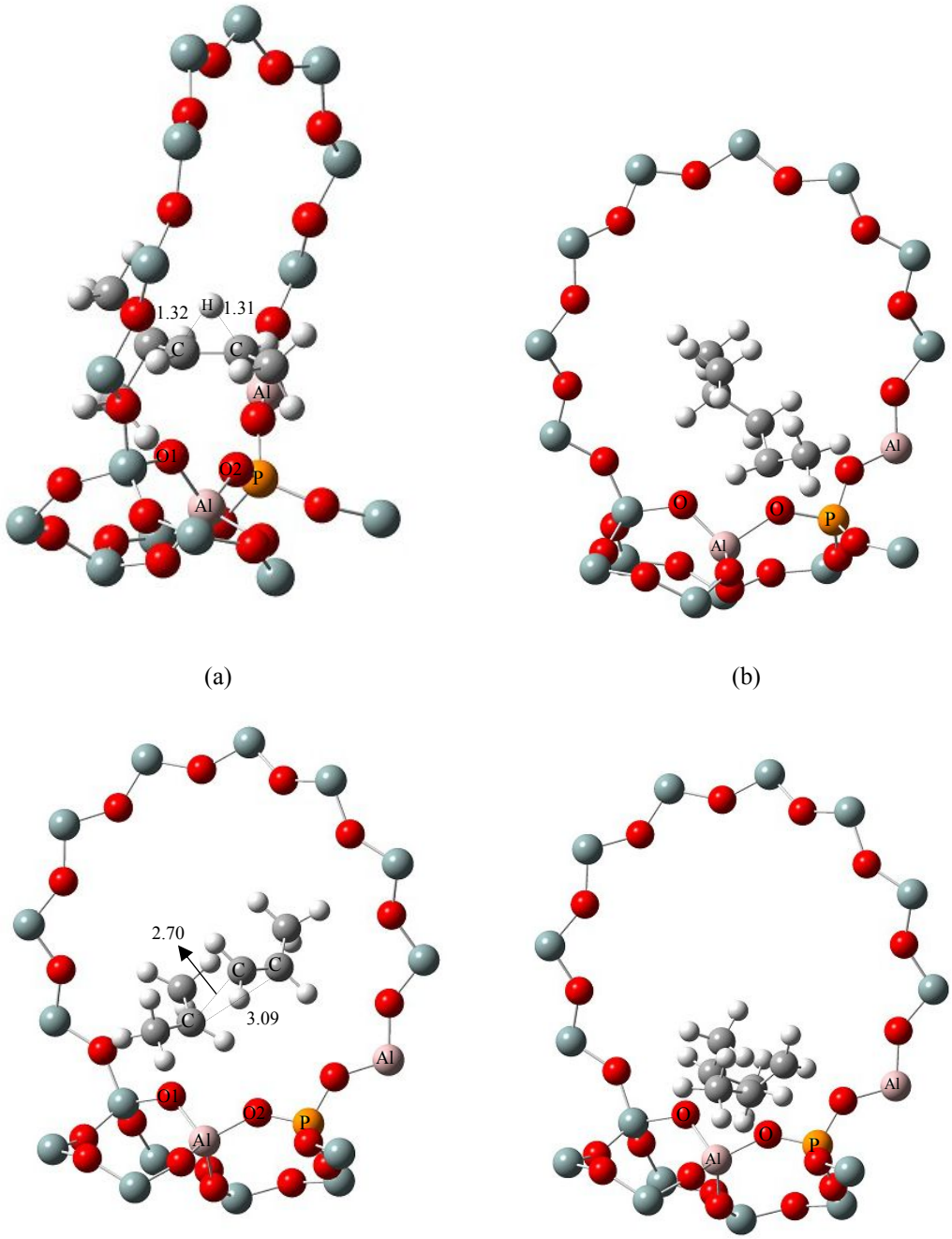

(a) (b)

(c) (d)

Fig. S29 Optimized structures of (a) TS-alkene-6, (b) INT-alkene-6, (c) TS-alkene-7, and (d) INT-alkene-7.

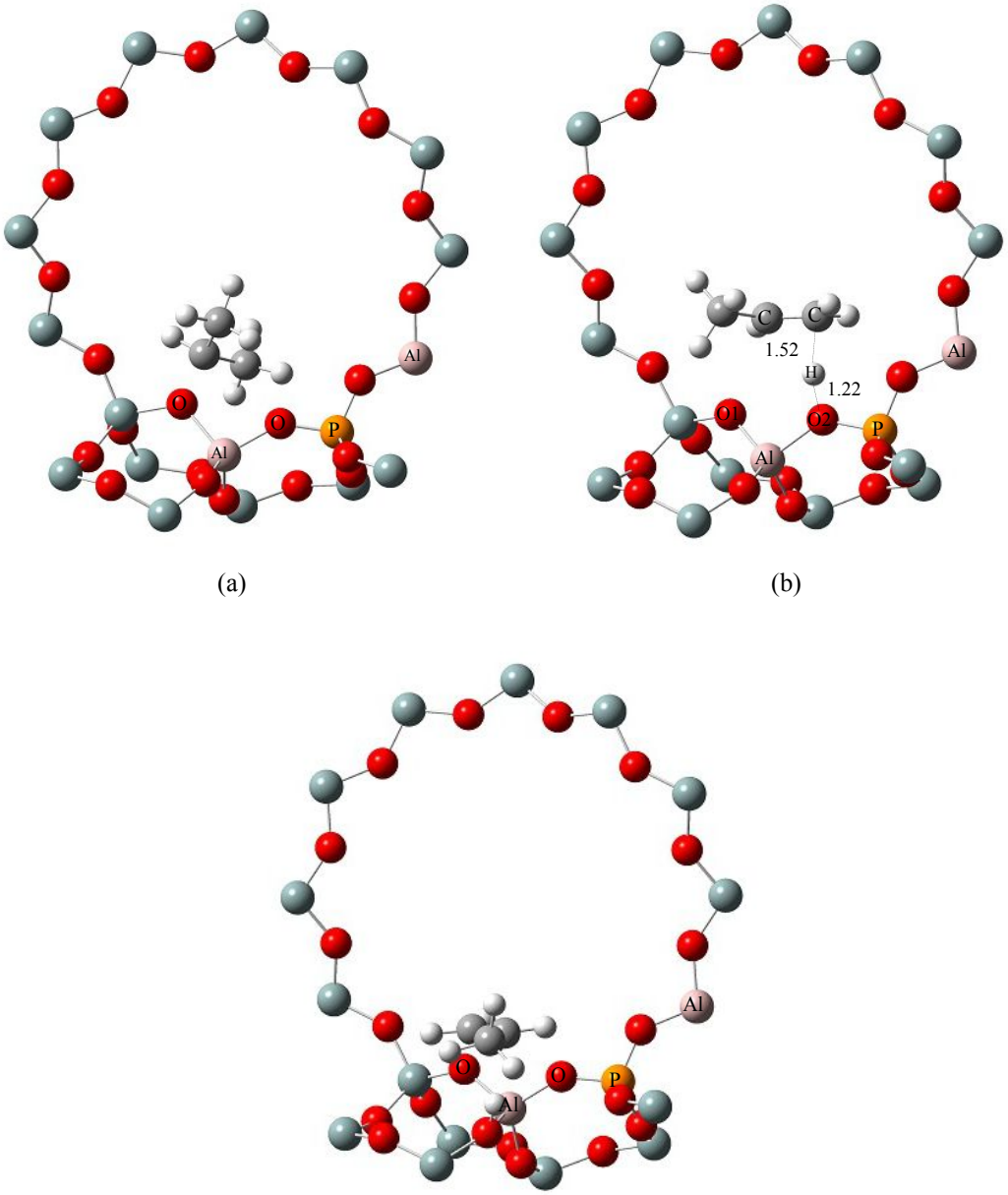

Fig. S30 Optimized structures of (a) INT-alkene-7-nopropene, (b) TS-alkene-8, and (c) propene.

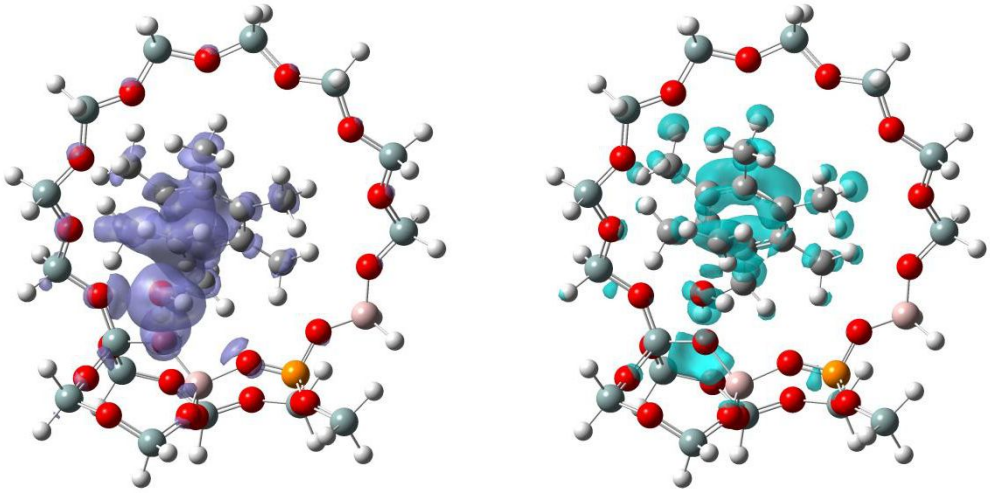

(a) (b)

Fig. S31 Difference charge densities for TS-direct-1. (a) positive DCD and (b) negative DCD.

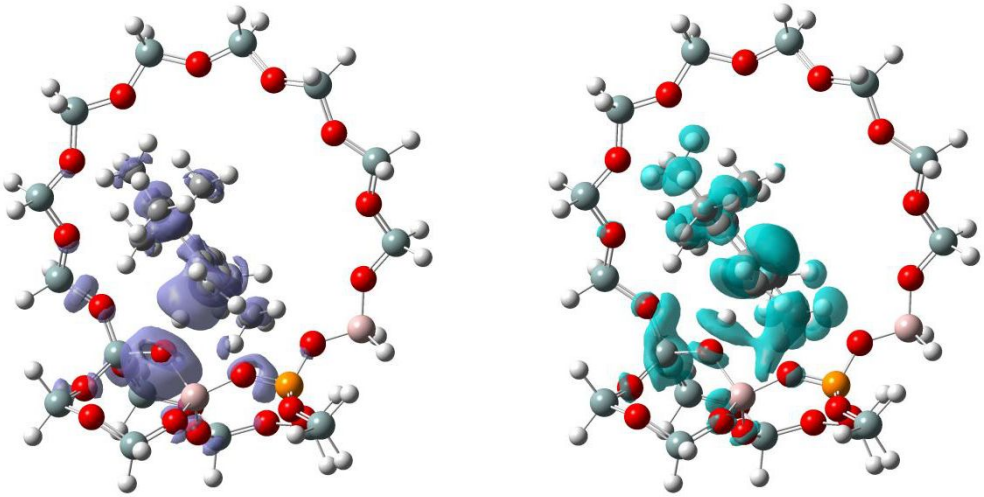

(a) (b)

Fig. S32 Difference charge densities for TS-direct-2. (a) positive DCD and (b) negative DCD.

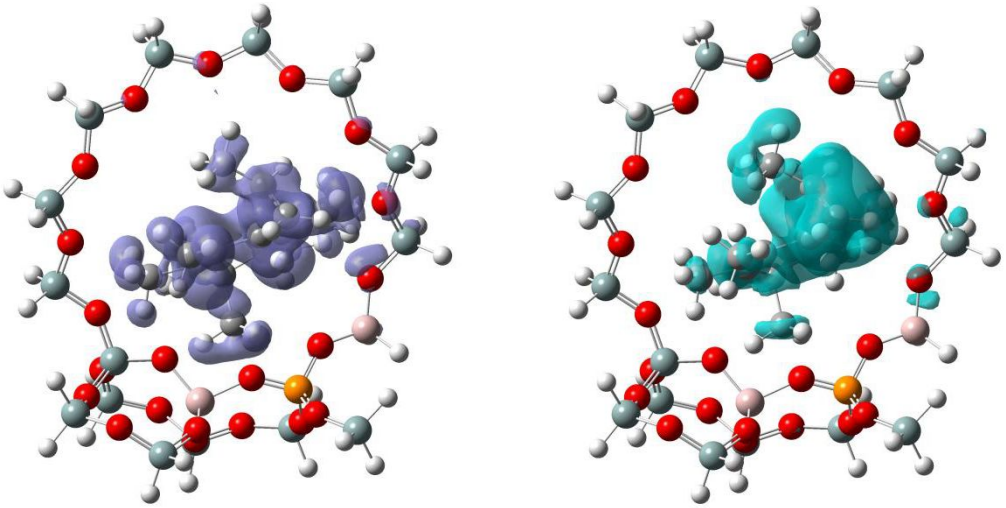

(a) (b)

Fig. S33 Difference charge densities for TS-direct-6. (a) positive DCD and (b) negative DCD.

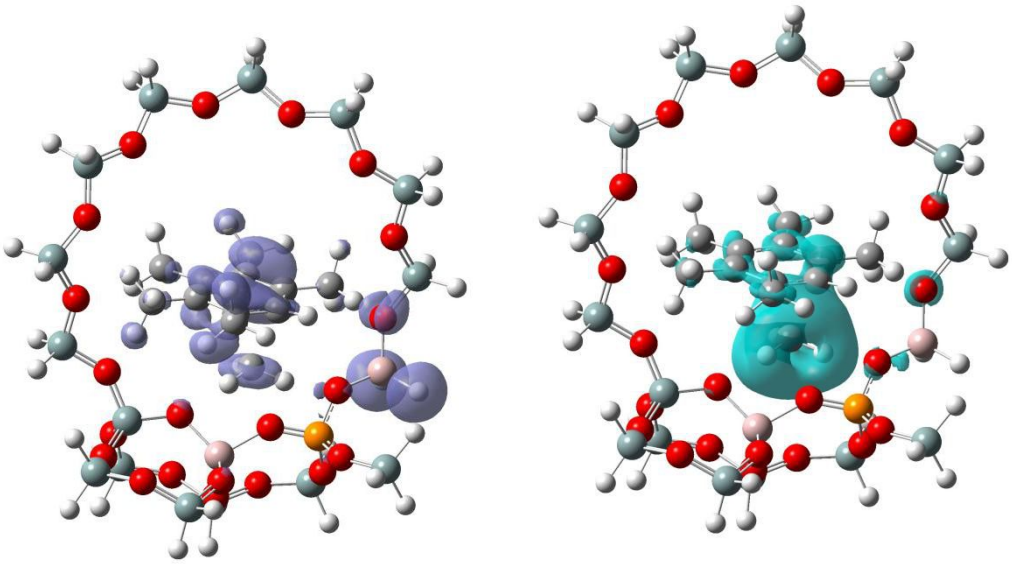

(a) (b)

Fig. S34 Difference charge densities for TS-direct-7. (a) positive DCD and (b) negative DCD.

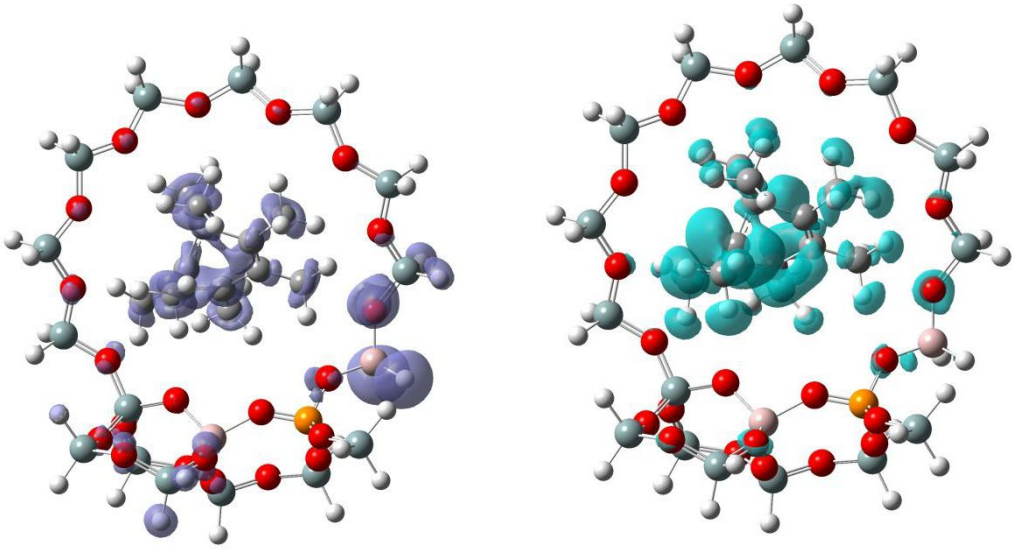

(a) (b)

Fig. S35 Difference charge densities for TS-paring-1. (a) positive DCD and (b) negative DCD.

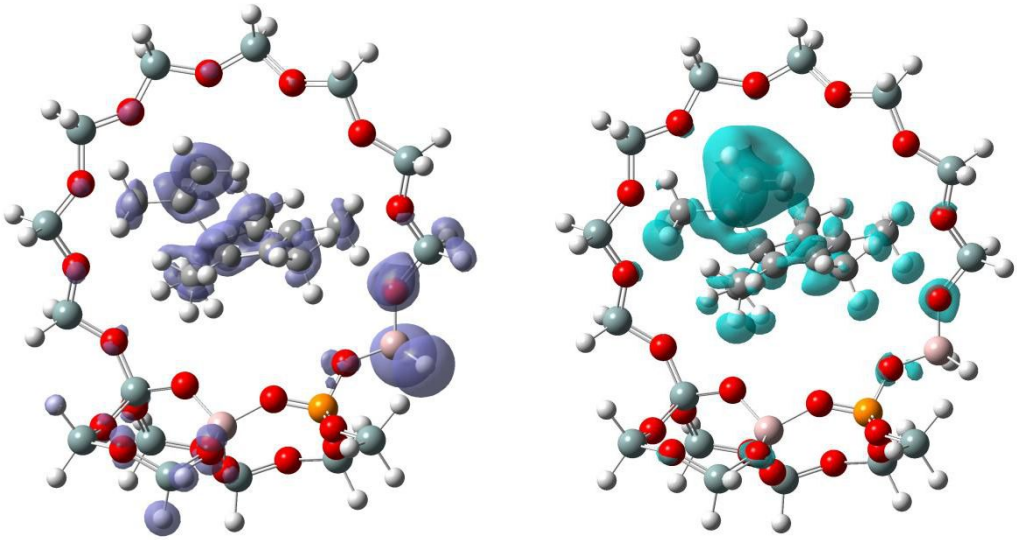

(a) (b)

Fig. S36 Difference charge densities for TS-paring-2. (a) positive DCD and (b) negative DCD.

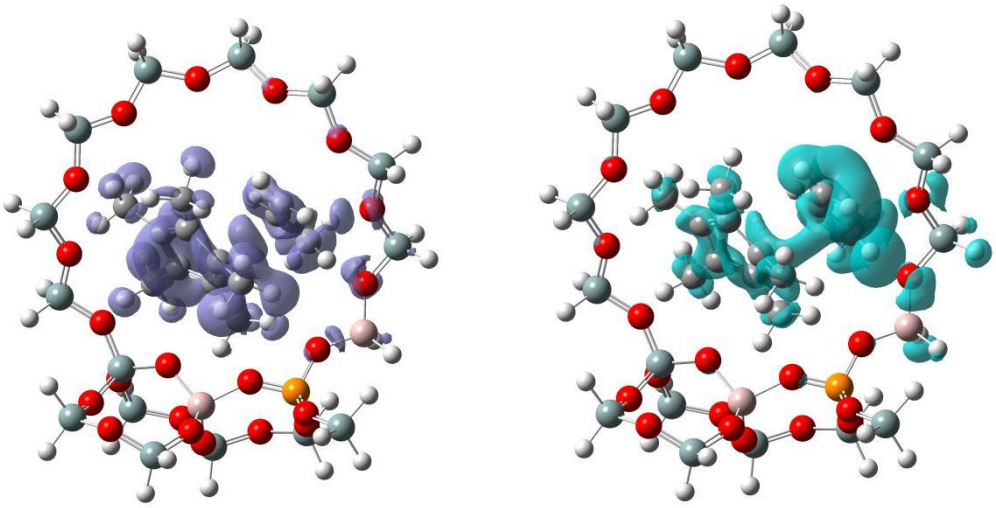

(a) (b)

Fig. S37 Difference charge densities for TS-paring-3. (a) positive DCD and (b) negative DCD.

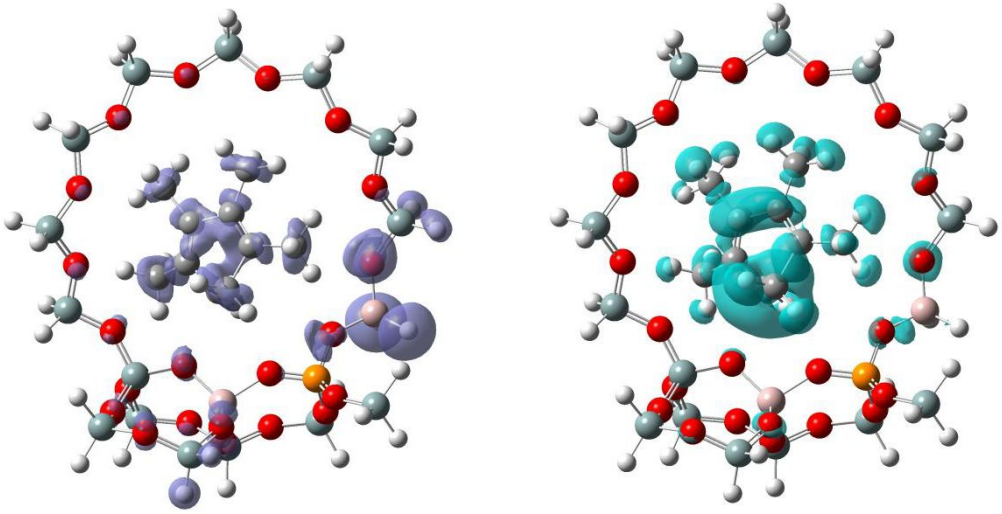

(a) (b)

Fig. S38 Difference charge densities for TS-paring-6. (a) positive DCD and (b) negative DCD.

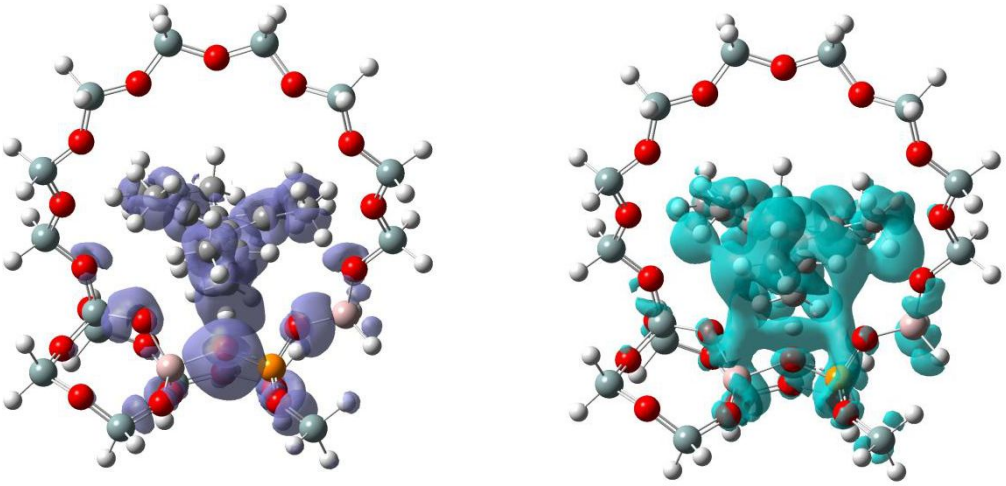

(a) (b)

Fig. S39 Difference charge densities for TS-spiro-1. (a) positive DCD and (b) negative DCD.

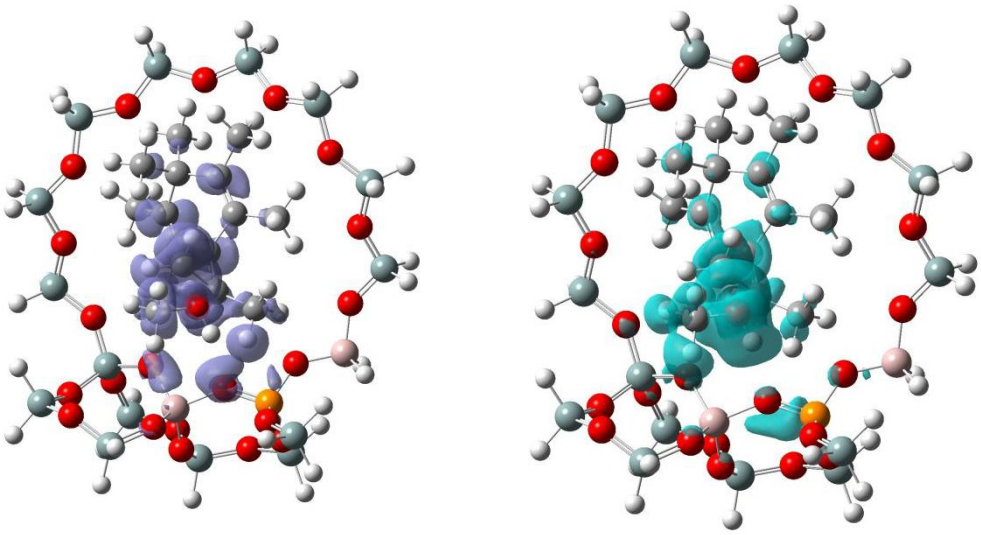

(a) (b)

Fig. S40 Difference charge densities for TS-spiro-1-CH_3OH. (a) positive DCD and (b) negative DCD.

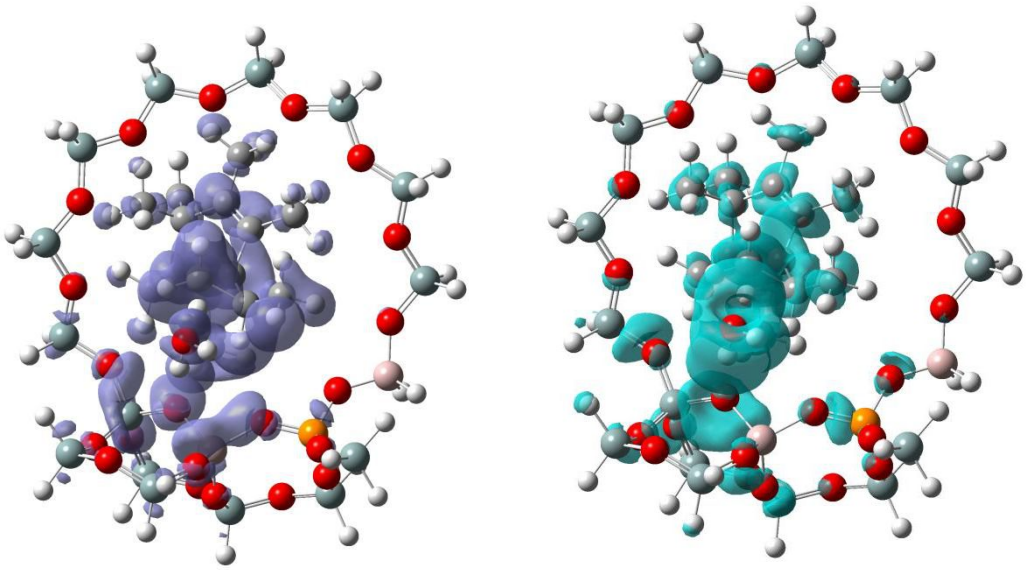

(a) (b)

Fig. S41 Difference charge densities for TS-spiro-1-H_2O. (a) positive DCD and (b) negative DCD.

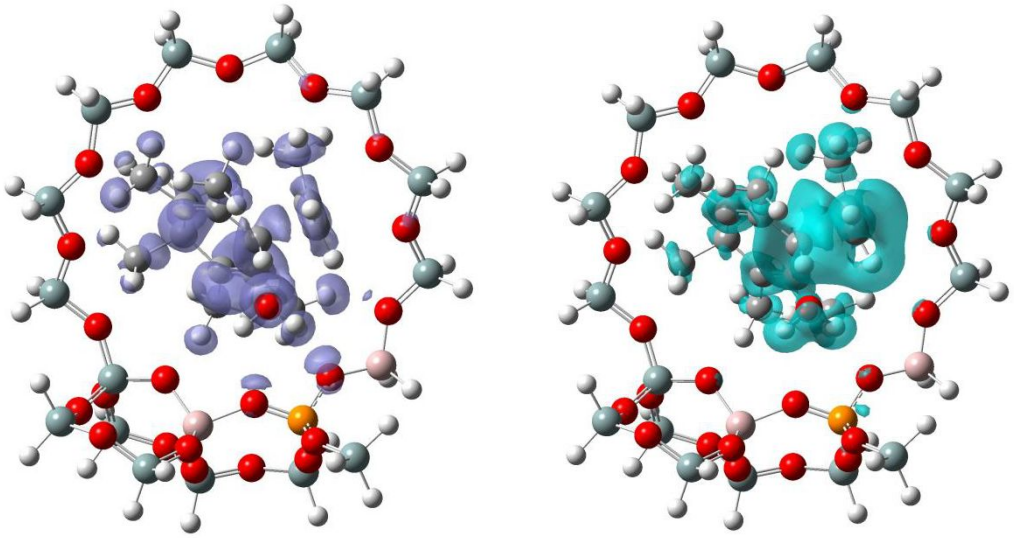

(a) (b)

Fig. S42 Difference charge densities for TS-spiro-2-H_2O. (a) positive DCD and (b) negative DCD.

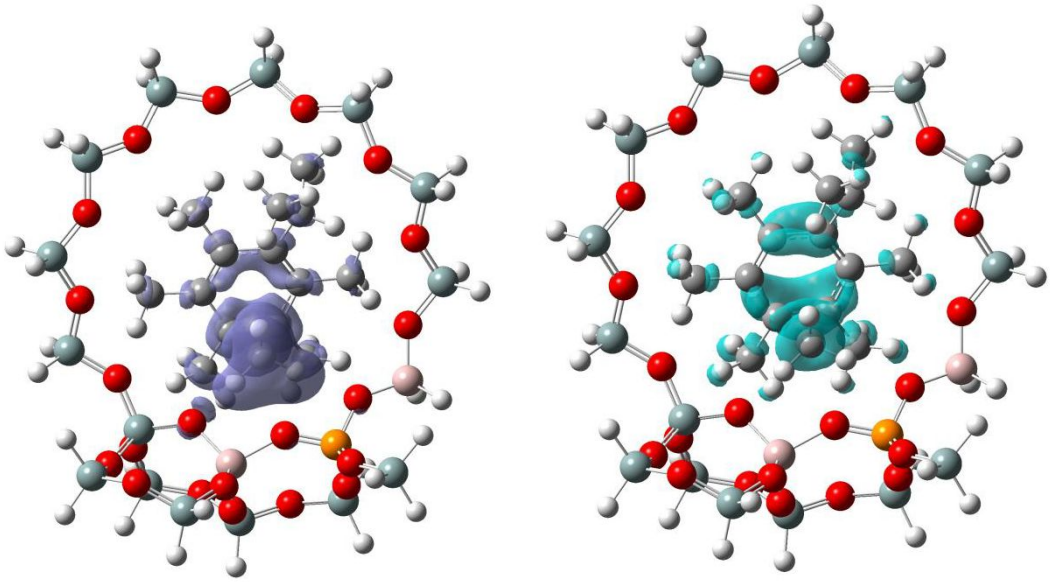

(a) (b)

Fig. S43 Difference charge densities for TS-ch3trans-1. (a) positive DCD and (b) negative DCD.

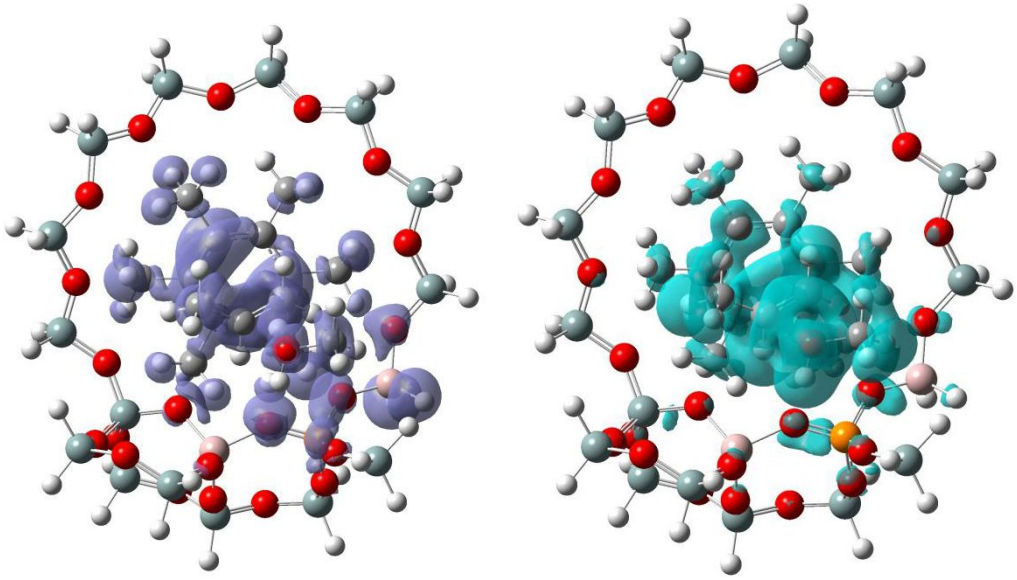

(a) (b)

Fig. S44 Difference charge densities for TS-ch3trans-4-CH_3OH. (a) positive DCD and (b) negative DCD.

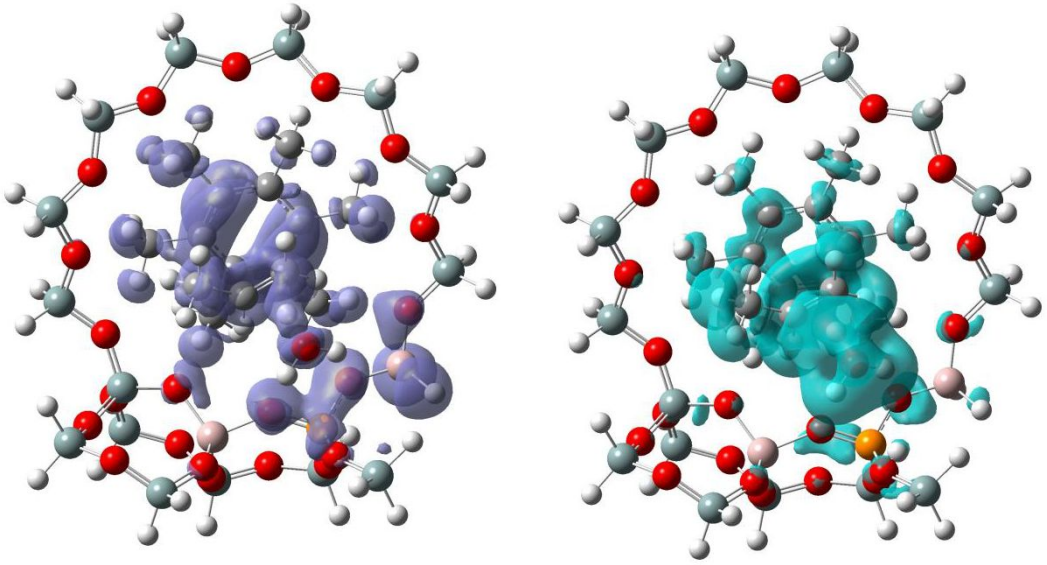

(a) (b)

Fig. S45 Difference charge densities for TS-ch3trans-4-H_2O. (a) positive DCD and (b) negative DCD.

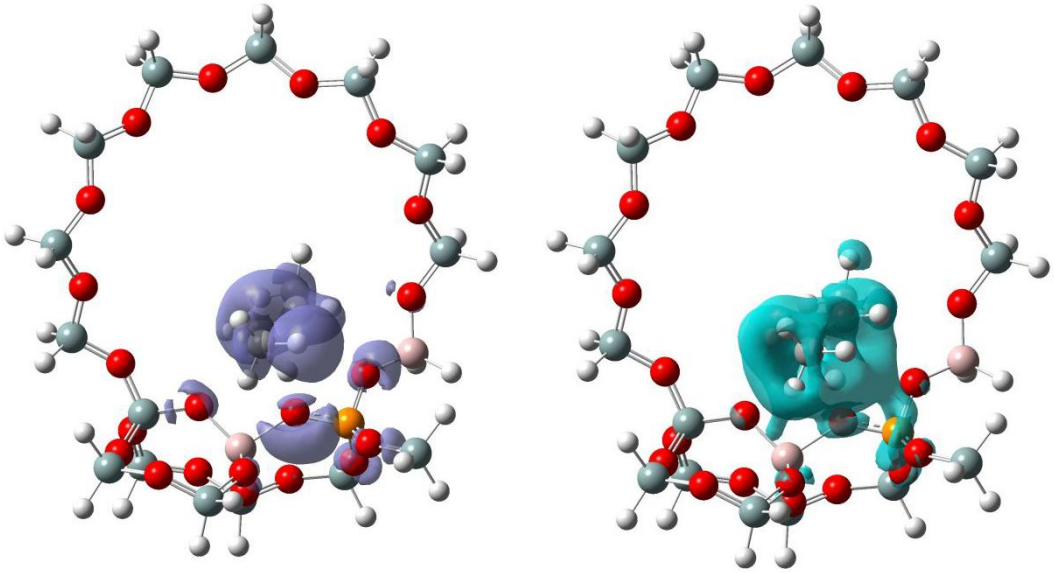

(a) (b)

Fig. S46 Difference charge densities for TS-alkene-2. (a) positive DCD and (b) negative DCD.

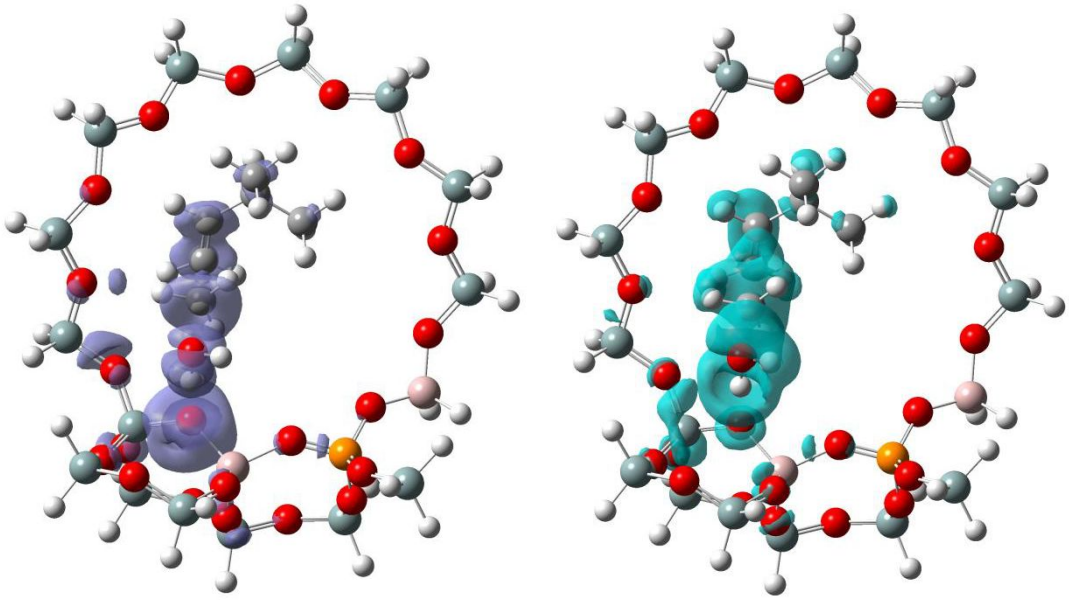

(a) (b)

Fig. S47 Difference charge densities for TS-alkene-5. (a) positive DCD and (b) negative DCD.

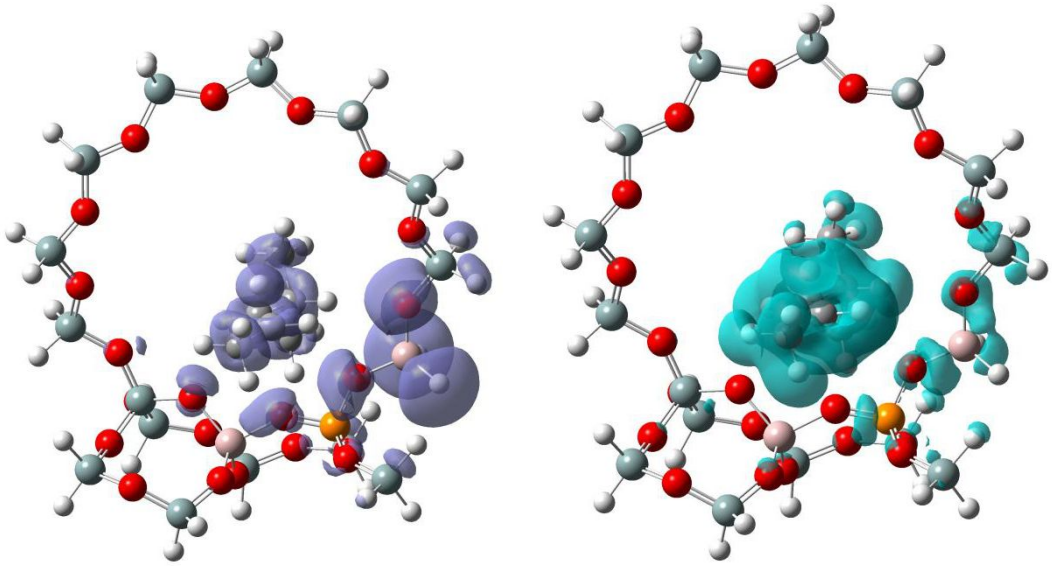

(a) (b)

Fig. S48 Difference charge densities for TS-alkene-6. (a) positive DCD and (b) negative DCD.

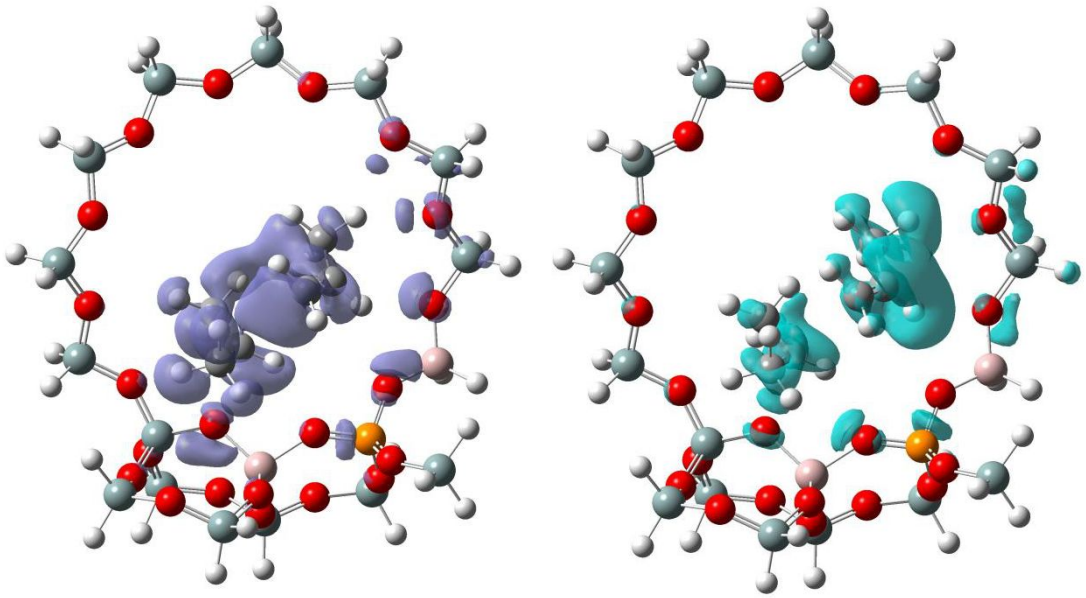

(a) (b)

Fig. S49 Difference charge densities for TS-alkene-7. (a) positive DCD and (b) negative DCD.

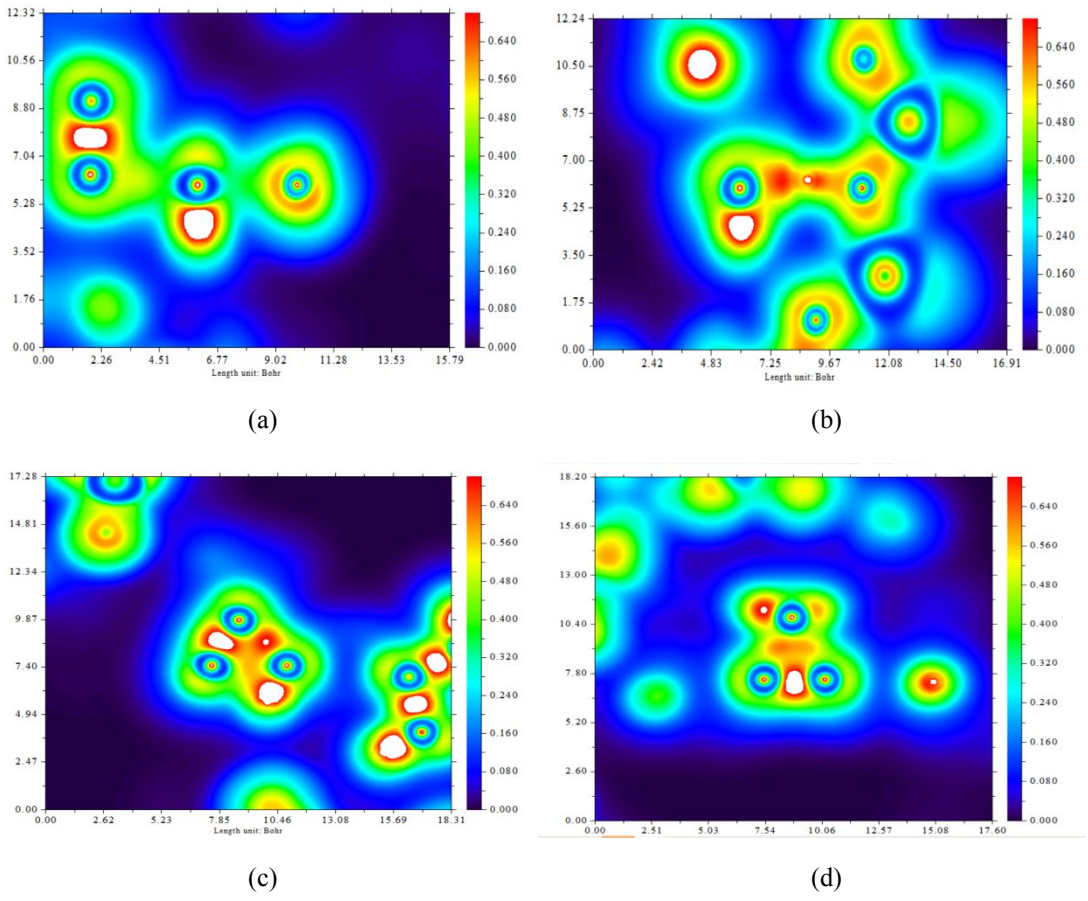

Fig. S50 Color-filled maps of (a, b, c, d) LOLs. (a) TS-direct-1, (b) TS-direct-2, (c) TS-direct-6, (d) TS-direct-7.

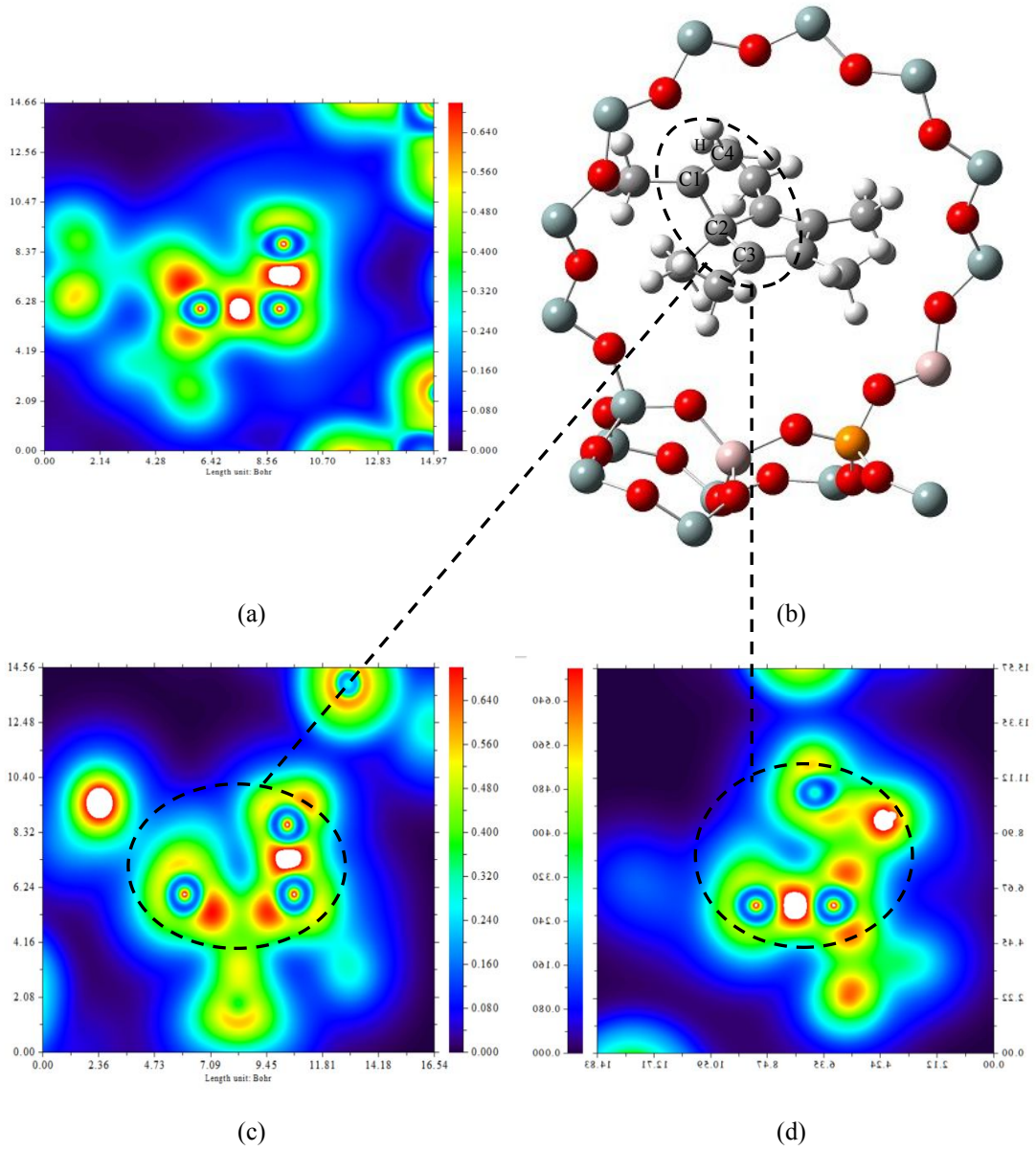

Fig. S51 Color-filled maps of LOL (a) TS-paring-1, optimized structure of (b) TS-paring-2, color-filled maps of LOLs for (c) TS-paring-2 (C1, C3, C4), and (d) TS-paring-2 (C2, C3, H).

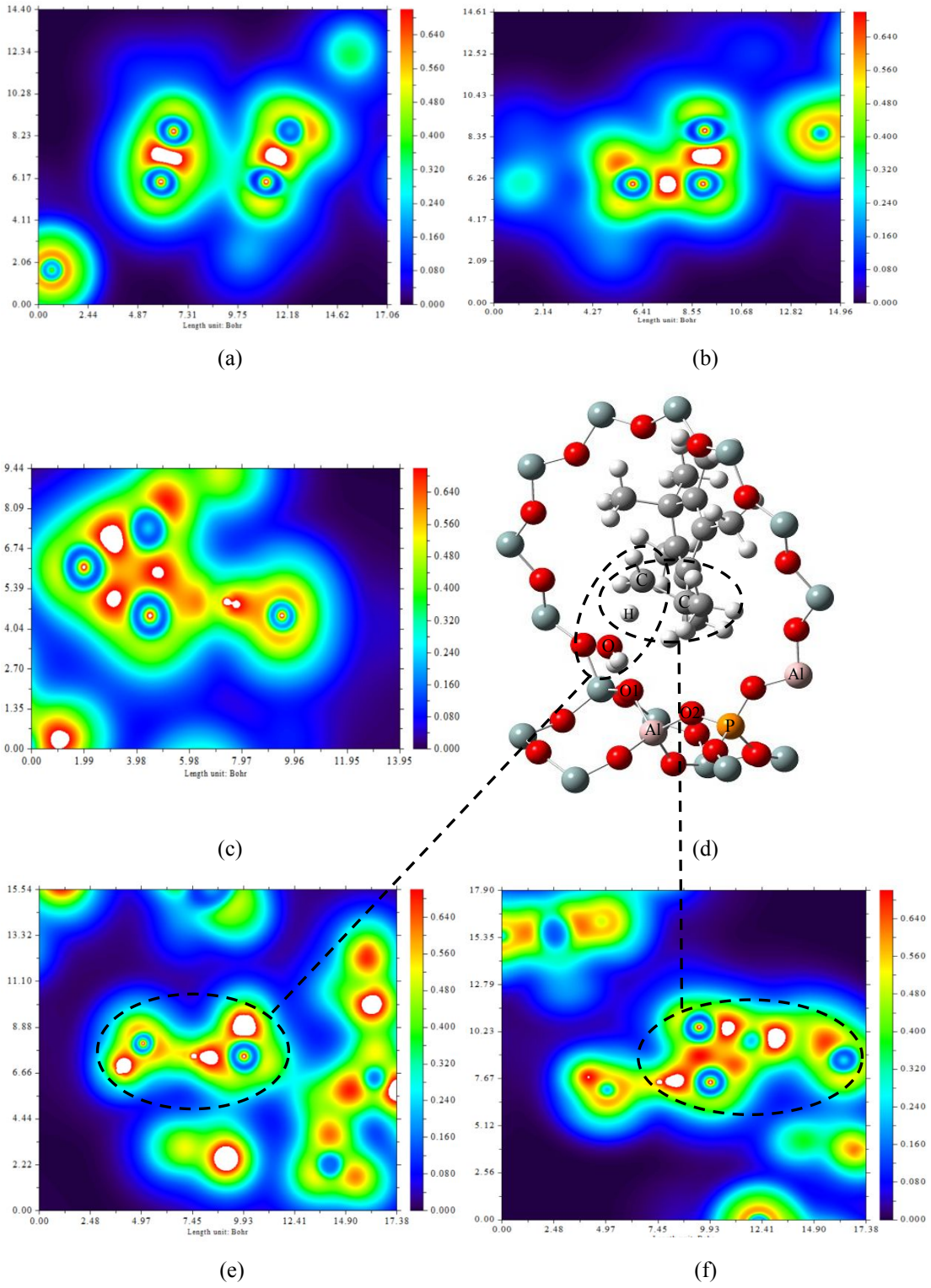

Fig. S52 Color-filled maps of LOLs. (a) TS-paring-3, (b) TS-paring-6, (c) TS-spiro-1, optimized structure of (d) TS-spiro-1-H_2O, color-filled maps of LOLs for (e, f) TS-spiro-1-H_2O.

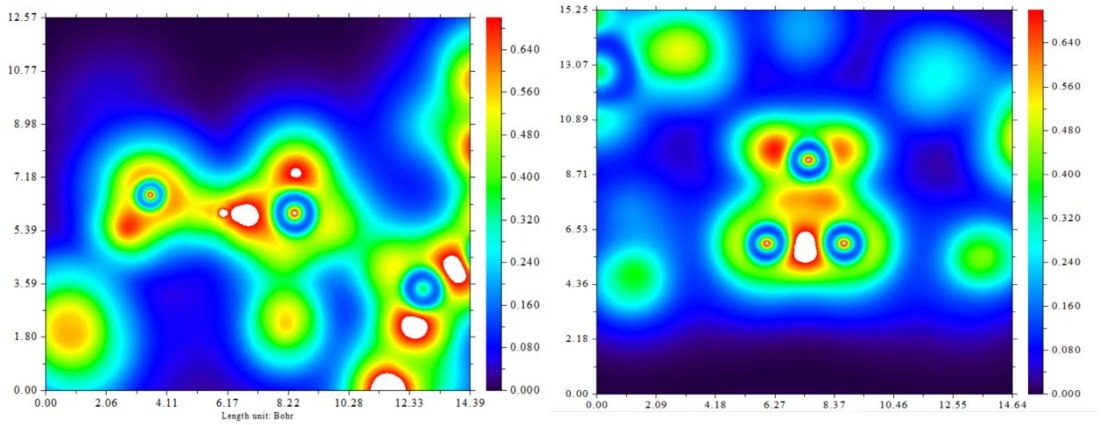

(a) (b)

Fig. S53 Color-filled maps of (a, b) LOLs. (a) TS-spiro-1-CH_3OH, and (b) TS-ch3trans-1.

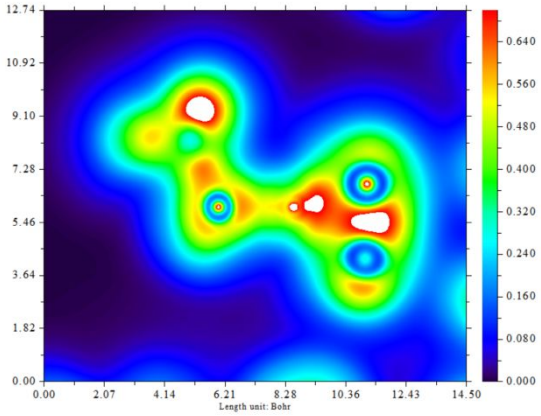

(a)

Fig. S54 Color-filled maps of LOLs. (a) TS-ch3trans-4-CH_3OH.

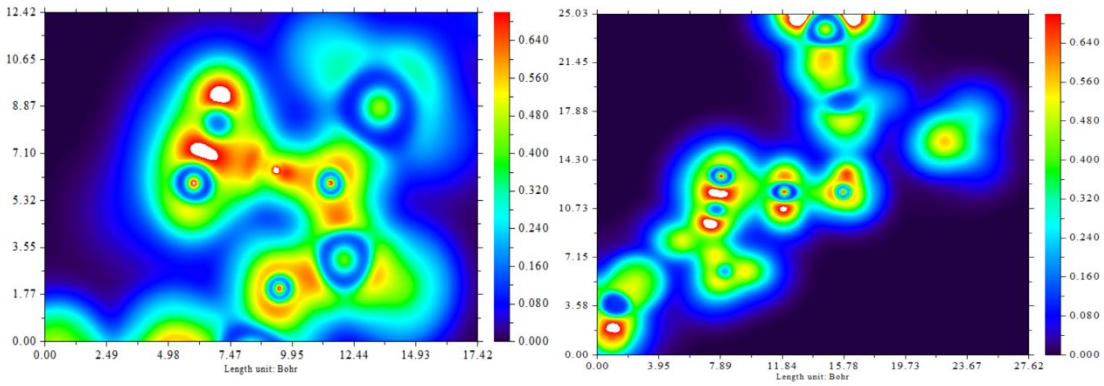

(a) (b)

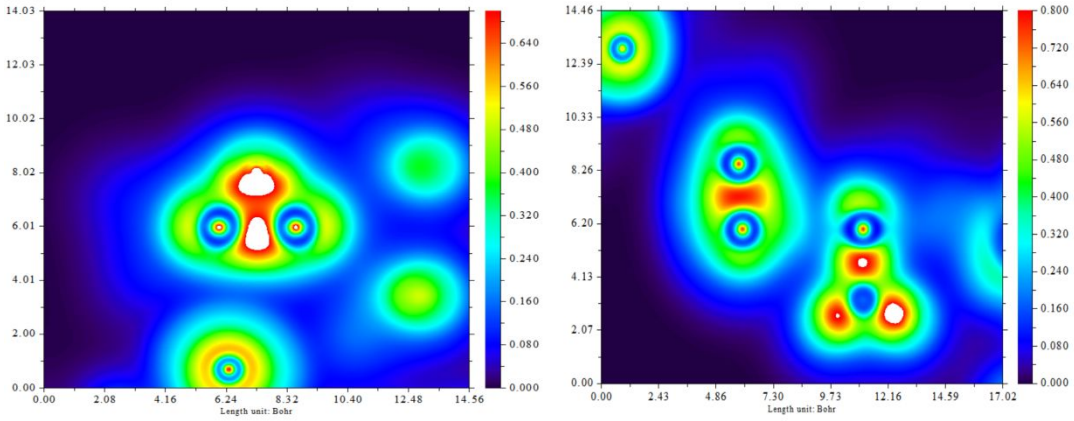

(c) (d)

Fig. S55 Color-filled maps of (a, b, c, d) LOLs. (a) TS-alkene-2, (b) TS-alkene-5, (c) TS-alkene-6, and (d) TS-alkene-7.

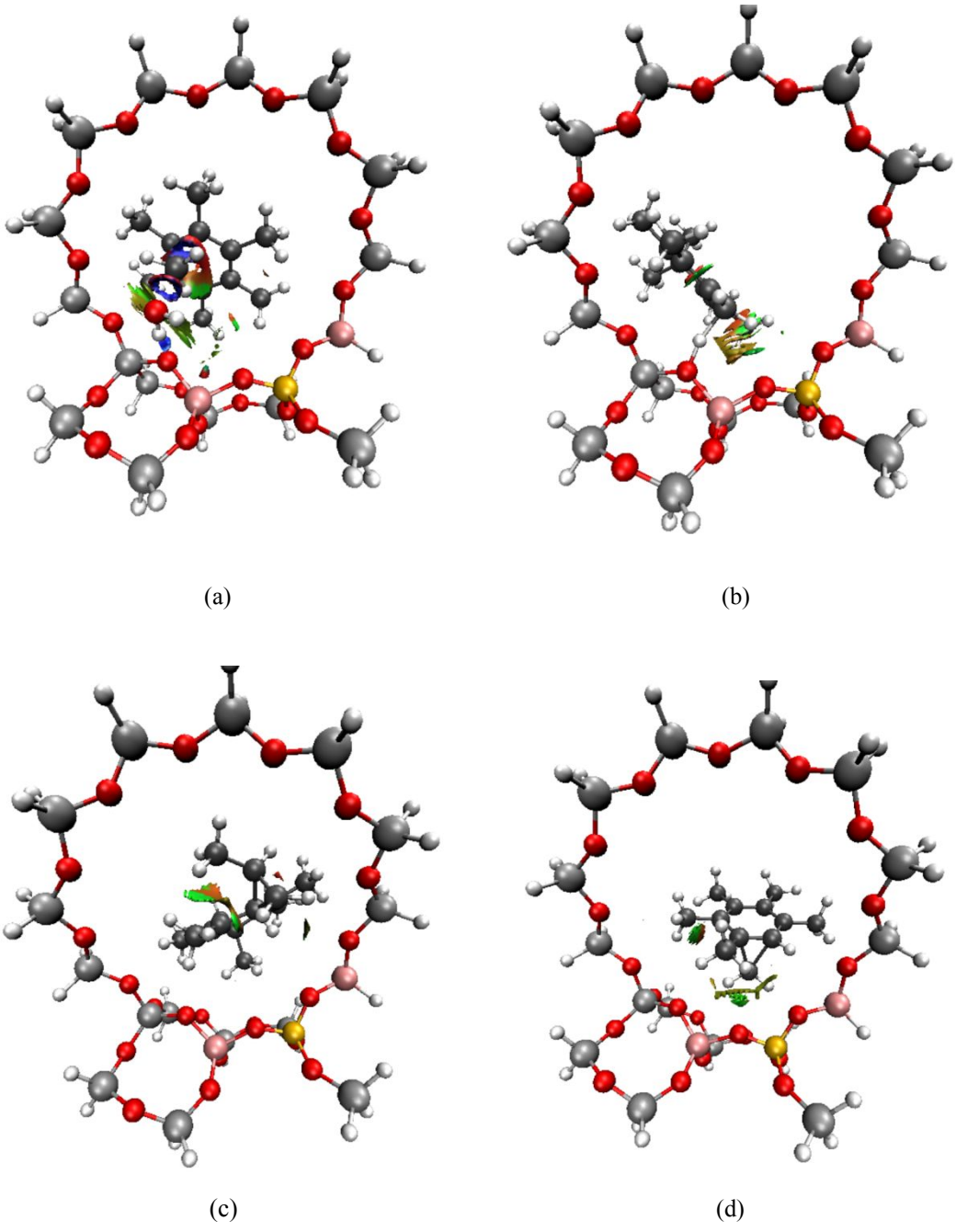

Fig. S56 Isosurface plots of (a, b, c, d) RDGs. (a) TS-direct-1, (b) TS-direct-2, (c) TS-direct-6, and (d) TS-direct-7.

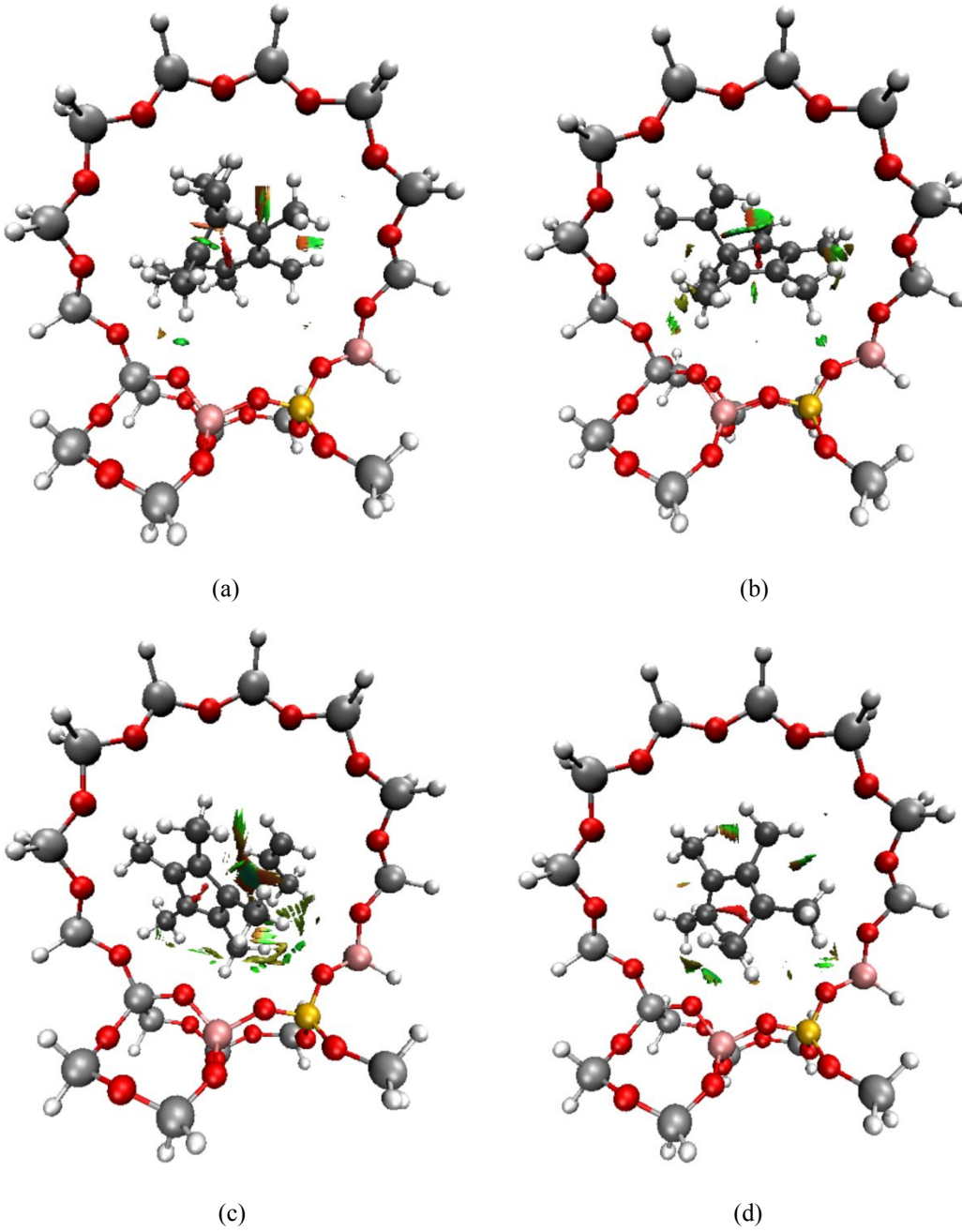

Fig. S57 Isosurface plots of (a, b, c, d) RDGs. (a) TS-paring-1, (b) TS-paring-2, (c) TS-paring-3, and (d) TS-paring-6.

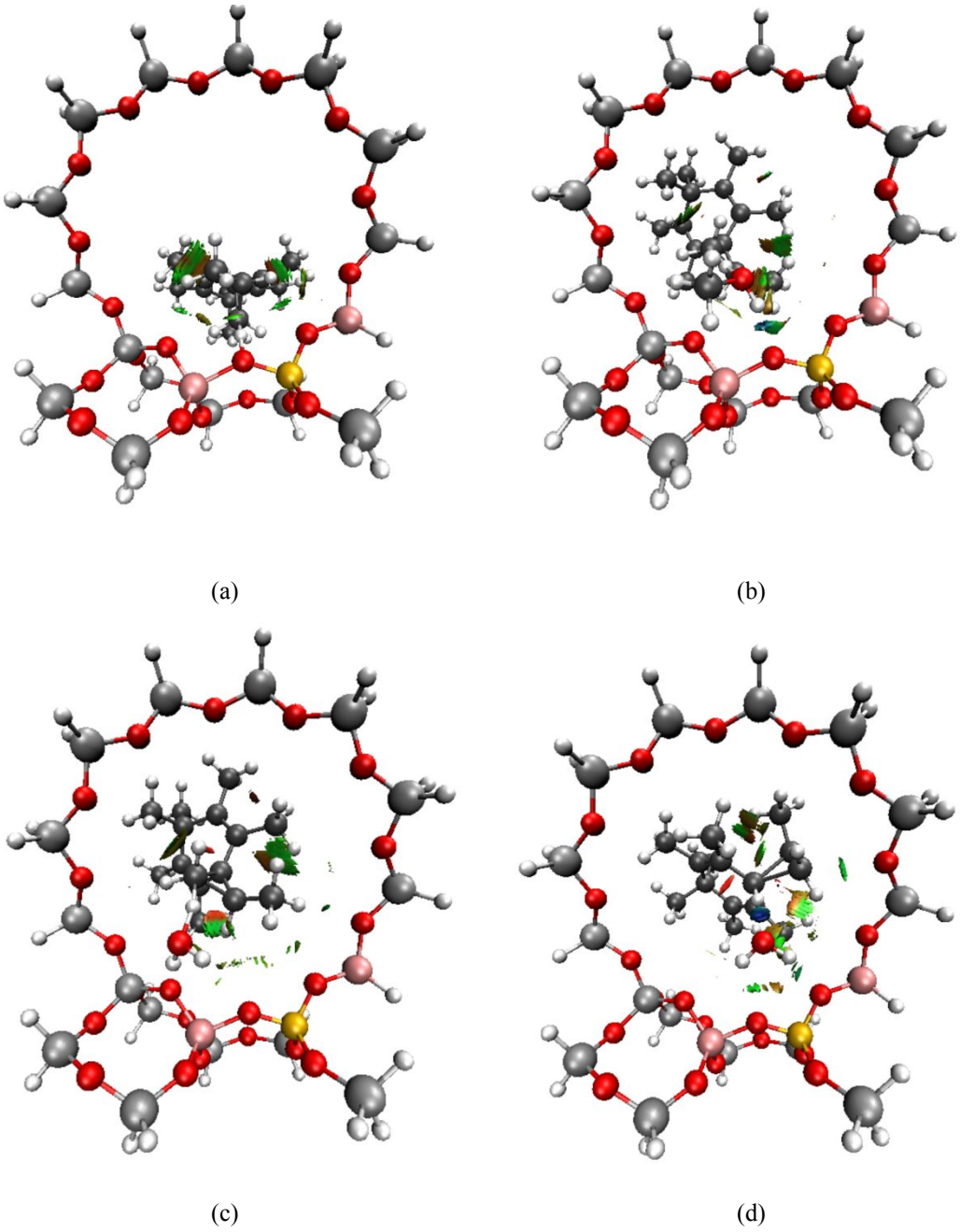

Fig. S58 Isosurface plots of (a, b, c, d) RDGs. (a) TS-spiro-1, (b) TS-spiro-1-CH_3OH, (c) TS-spiro-1-H_2O, and (d) TS-spiro-2-H_2O.

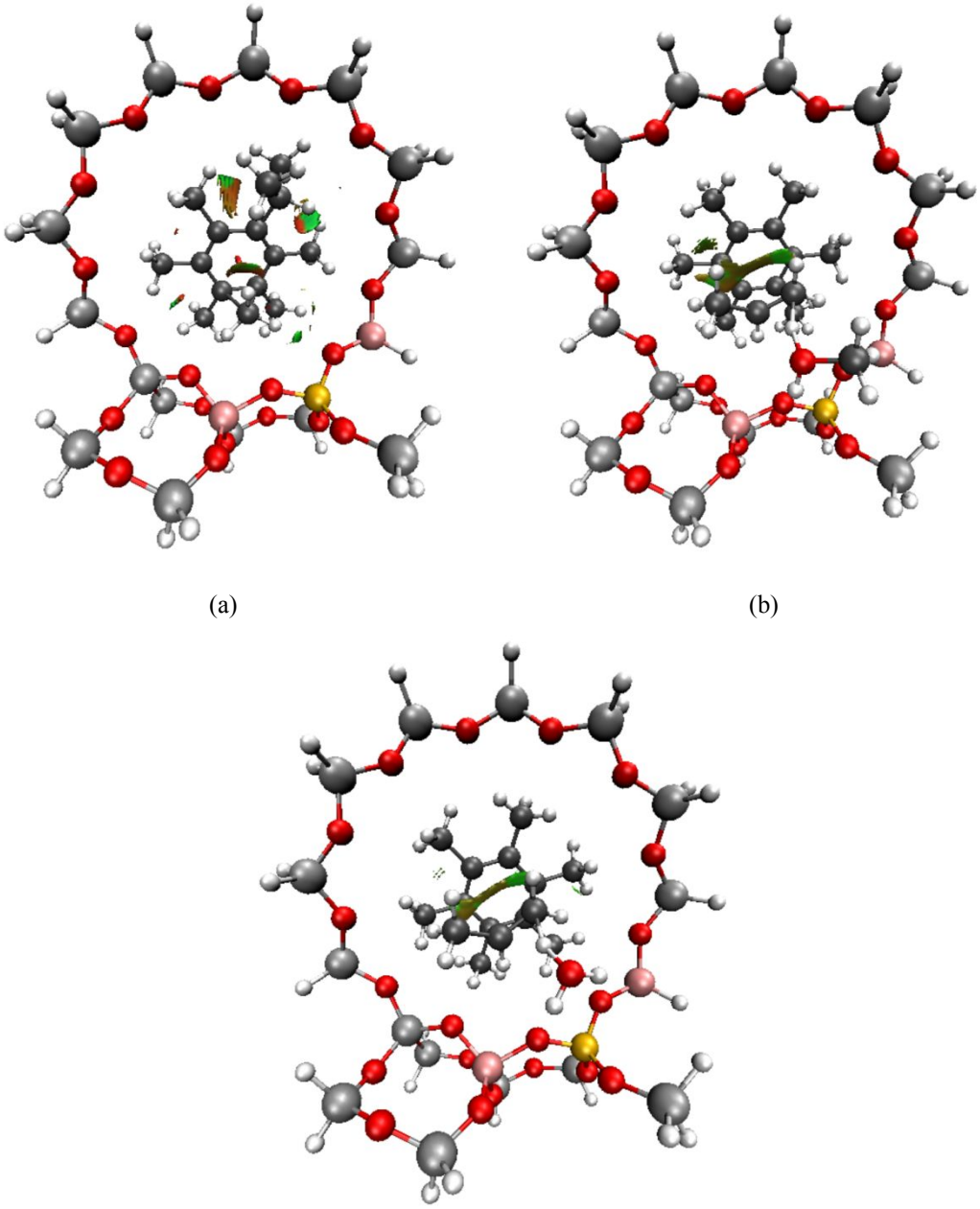

(a) (b)

(c)

Fig. S59 Isosurface plots of (a, b, c) RDGs. (a) TS-ch3trans-1, (b) TS-ch3trans-4-CH_3OH, and (c) TS-ch3trans-4-H_2O.

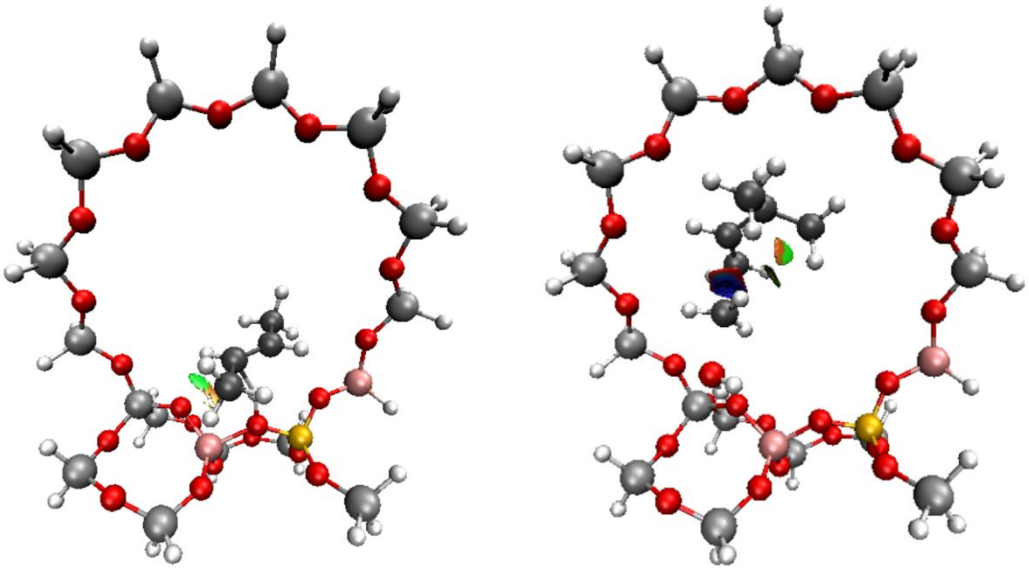

(a)

(b)

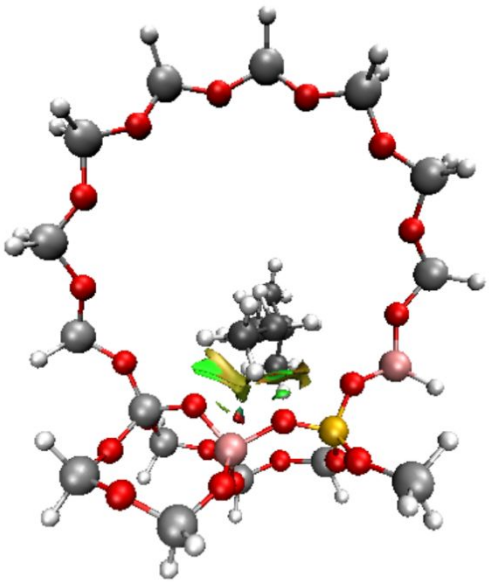

(c)

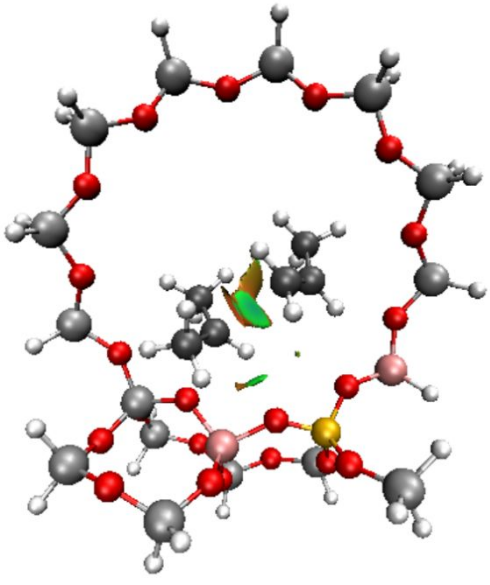

(d)

Fig. S60 Isosurface plots of (a, b, c, d) RDGs. (a) TS-alkene-2, (b) TS-alkene-5, (c) TS-alkene-6, and (d) TS-alkene-7.

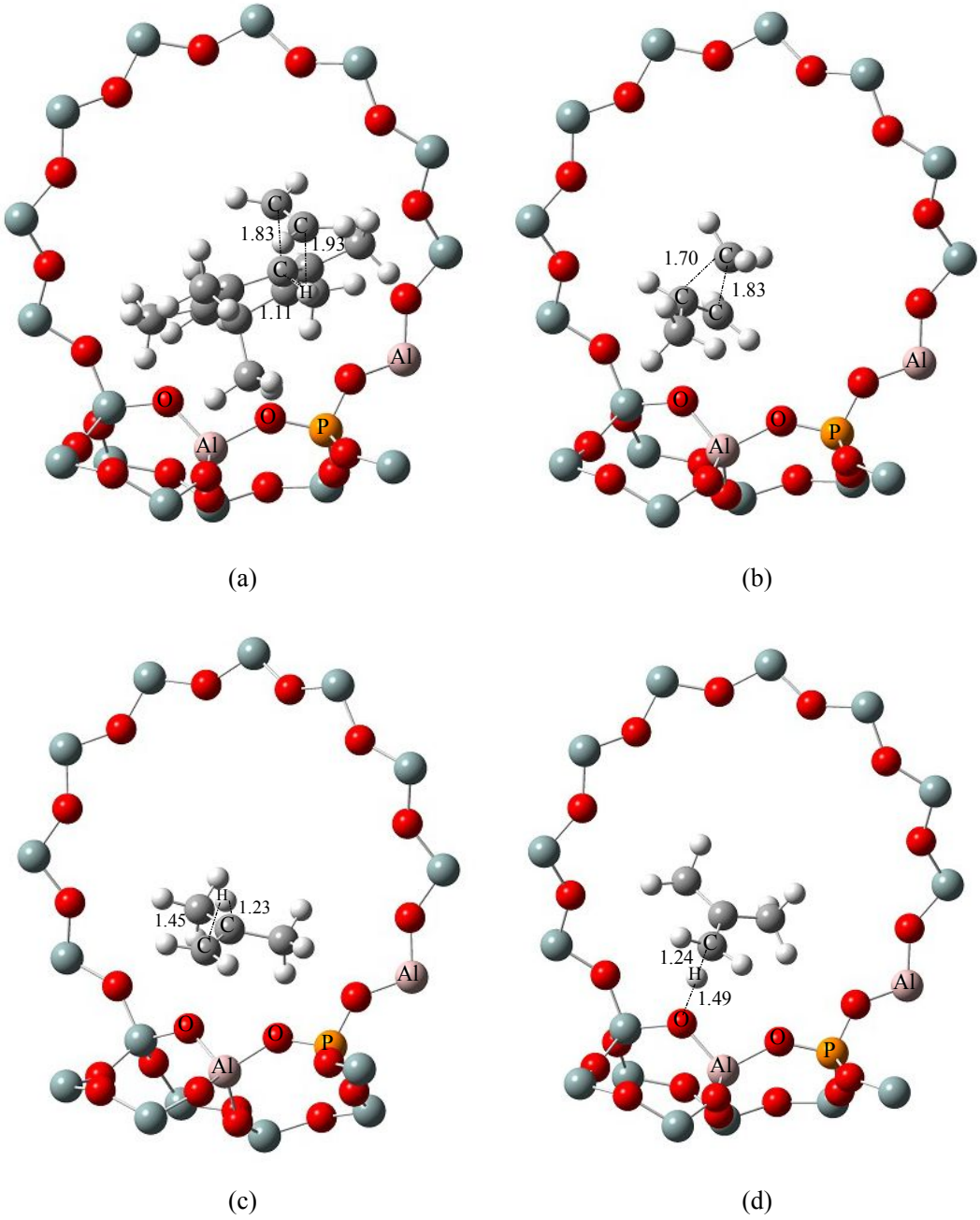

Fig. S61 Optimized structures of (a) TS-direct-ethene, (b) TS-isobutene-1, (c) TS-isobutene-2, and (d) TS-isobutene-3.